Memoirs of the School of Engineering, Nagoya University
Vol.48, No.1 (1996)

ON THE VIBRATIONS OF A SHAFT PASSING THROUGH ITS CRITICAL SPEED

Hiroshi OTA, Shin-ichiro NAKAMURA and Masayoshi KATO*

Department of Mechanical Engineering

(Received May 31, 1996)

Abstract

In this paper, we analyse whirling vibration and torsional vibration of a rotating shaft after passing through its critical speed for whirling. First, equations of motion for a rotor-shaft system are derived with accuracy to the second-order of shaft deformations, and it is demonstrated that Euler's equations of motion are equivalent to Lagrange's equations of motion. Then we deals with the passage problem of a rotor-shaft system under a constant driving torque. And analyses for our equations of motion show that the torsional vibration of a rotating shaft can be caused after passing its critical speed for whirling, and the vibration is discussed in both cases of symmetrical rotor and asymmetrical rotor.

Keywords: vibration of rotating body, Euler's equations of motion, Lagrange's equations of motion, symmetrical rotor, asymmetrical rotor, whirling, torsional vibration, critical speed, resonance, numerical solution, asymptotic method

Contents

*Faculty of Education, Aichi University of Education

NOTATION

A	amplitude of shaft whirling
A_k	amplitude of vibration mode whirling with frequency p_k
c_1, c_2, c_3	viscous damping coefficients for translation, inclination and rotation of rotor
e	eccentricity of rotor
$I = (I_1 + I_2)/2$	mean moment of inertia of rotor about two principal axes of inertia perpendicular to polar axis
I_1, I_2	moments of inertia of rotor about two principal axes of inertia perpendicular to polar axis (let $I_1 > I_2$)
Im[ ]	complex component in [ ]
I_p	moment of inertia of rotor about rotating shaft
$i = \sqrt{-1}$	unit of imaginary number
$l = \overline{AB}$	length of shaft
l_1	distance from driving point A to point S which carries rotor
$l_2 = l - l_1$	distance from point S to another shaft end B
m	mass of rotor
p_1, p_2, p_3, p_4	natural angular frequencies for whirling of shaft ($p_1 > p_2 > p_3 > p_4$)
p_t	natural angular frequency of torsion of shaft
T_r	driving torque
t	time
x, y	x- and y-components of shaft deflection at point S
x_1, x_2, x_3	three principal axes of inertia of rotor
$z = x + iy$	shaft deflection expressed in complex number
α, γ, δ	spring constants for shaft deflection
δ_t	spring constant for torsion of shaft between driving point A and point S
η	angular position of dynamic unbalance
λ	angular acceleration at shaft end A
ω	rotating speed at point S
ω_a	rotating speed at point A
ω_{ac}	critical speed for shaft whirling
τ	dynamic unbalance of rotor
θ_t	angle of shaft torsion between A and S
θ_{t1}	component of θ_t changing monotonously with time
$\theta_{t2} = \theta_t - \theta_{t1}$	vibratory component of θ_t
θ_{t2max}	maximum value of θ_{t2} in one acceleration/deceleration
θ_x, θ_y	projection of inclination angle of shaft to xz- and yz-planes
$\theta_z = \theta_x + i\theta_y$	inclination angle of shaft expressed in complex number
ξ	angular position of eccentricity
$\Delta I = (I_1 - I_2)/2$	difference of I_1 and I_2 from mean value I
$\Delta I/I$	asymmetry of rotor
Φ_k	phase angle of vibration mode whirling with frequency p_k
Θ	rotating angle of shaft at point S
Θ_a	rotating angle of shaft at point A
$\bar{}$	complex conjugate
$\dot{}$	differential with respect to time

Chapter 1. General Introduction

Nowadays, rotating machines are much larger than as they were in the past and are operated in higher rotating speed for highest performance. For higher rotating speed, not only a large vibration but also even a small vibration of the rotor-shaft system must be removed. In order to prevent such vibrations, we should know what vibrations appear in the system, the mechanisms how they occur, and how we can remove or reduce these vibrations.

There have been a large number of studies on the rotor-shaft system and its vibration since Rankine[1], Grammel[2], Stodola[3], and Den Hartog[4] reported on natural frequencies and major critical speed. And recently reported on vibrations in passing critical speed[5-9], vibrations of shaft having different stiffness[10-12], vibrations of asymmetrical rotor-shaft system[13-19], vibration of a rotating shaft with non-linear spring constants[20-22], vibrations of a rotating shaft with different pedestal stiffness[22-25], vibrations of a rotating shaft having a crack[26], vibration of rotor-shaft system with variable rotating speed[27-28], vibration of a rotating shaft driven by a universal joint[29-33], acceleration patterns with consideration of torsional vibration of the rotating shaft[34], and balancing the rotor-shaft system. By helps of these investigations, rotating machines can be driven smoother than before.

To analyse theoretically the passage problem of critical speed, as well as other problems of rotor-shaft system, the equations of motion is very important. There are two major methods of deriving equations of motion, one is the Lagrange's method and the other is Euler's one. These two methods must be equivalent at least for vibration problems of rotating bodies, but sometimes they provide different appearance of equations of motion[19,28,35,36]. In chapter 2, we analyse why this occurs by equations with precision of second-order of shaft deformation. Using the theory of elastics on bending and torsion of the shaft[37], equations of motion of rotor-shaft system with variable rotating speed are derived by both methods[38]. The result shows that both two methods are really equivalent, and that the lack of second-order of small quantities of shaft deformations causes the difference in the derived equations.

In the field of passage problem of major critical speed, there are a large number of studies about the system consisting of symmetrical rotor and symmetrical shaft[7,39,40]. There are some studies about the system consisting of symmetrical rotor and asymmetrical shaft[41-44] or the system consisting of asymmetrical rotor and symmetrical shaft[18], but they are much smaller in number than the former symmetrical-symmetrical system. A system with an asymmetrical shaft is similar to a system with asymmetrical rotor, both of which have unstable areas near their critical speeds. If asymmetry of the shaft is smaller than a certain value, some angular positions of dynamic unbalance make the maximum amplitude of whirling smaller than that in case of a system having symmetrical rotating shaft[44].

Ota et al[18] analysed the vibration of asymmetry rotor-shaft system in passing through the critical speed under constant angular acceleration and explained why the maximum amplitude of shaft whirling may be smaller than that in the case of symmetrical rotor-shaft system. It is because the maximum amplitude of whirling depends not only on eccentricity, dynamic unbalance, and asymmetry of rotor but also on their relative angular positions. But the minimum driving torque for passing the critical speed is not discussed in detail, though the system may not pass the critical speed because of too large whirling amplitude caused by smaller driving torque. A rotor-shaft system driven under a larger driving torque passes through its critical speed smoothly like a system under constant angular acceleration. But smaller driving torque makes whirling amplitude in 'approaching' its critical speed too large, the system needs more driving torque for 'passing' the critical speed. Thus, in asymmetrical rotor-shaft system the effects of driving torque, asymmetry of rotor, eccentricity, and dynamic unbalance on the whirling amplitude of shaft and rotating speed should be

investigated. Especially under constant driving torque, the change of rotating speed and whirling amplitude must be known. What will happen in the system if the system cannot pass the critical speed? We consider this problem in chapter 3 by numerical analyses with using asymptotic method[45].

When a rotor-shaft system has just passed its critical speed for whirling, the amplitude of shaft whirling changes periodically, and its frequency of the change becomes higher as the system gets apart from the critical speed. The phenomenon like beats is already well-known[6-8], but our analyses show that this phenomenon may cause torsional vibration[46,47].

It may be considered that torsional vibration of rotating shaft seems to occur in such systems that have gears or universal joints[48-50] or in systems of fluctuating driving torque[51,52]. And some researches are made by Tondl[53], for example, on a simple system consisting of a symmetrical rotor and symmetrical shaft with both ends fixedly supported. Gasch and Pfützner[54] investigated the minimum driving torque to pass through its critical speed for whirling, while no consideration was made about torsional vibration of the shaft.

Reciprocal engines such as ones for automobiles have periodical changes of torque working on their crank shaft[51,55]. And Ono[52] reported that a rotating shaft with constant speed ω has another vibration component with frequency $\omega \pm \nu$ when its driving torque is changed with frequency ν.

And in order to take fatigue of shaft into consideration, shafts with variable rotating speed, such as ones passing through their critical speed, experience whirling vibration with the frequency of which differs from that of shaft rotation, then the shafts undergo cyclic stress. In addition to whirling vibration, torsional vibration of shaft makes the shaft more dangerous in fatigue. Thus it is very important for safety and maintenance of machinery to consider whether the torsional vibration will occur in passing through critical speed and how large it will be if it occurs. Numerical analyses are made for symmetrical rotor-shaft system in chapter 4.

In asymmetrical rotor-shaft system, there are two frequency components of shaft whirling. One is observed even in symmetrical system and the other appears only in asymmetrical system. Then the system may resonate in shaft torsion at two rotating speeds. The character of these torsional vibration are investigated in chapter 5 by using asymptotic solutions[45].

The contents of this paper are as follows:

Chapter 1 deals with this general introduction as written above.

Chapter 2 describes the reason why equations of motion with variable rotating speed differ owing to being derived by Euler's method or Lagrange's method, and proves these two methods are essentially equivalent unless the precision of small quantities of second-order of shaft deformation is lost in their deriving process[38].

Chapter 3 shows the characteristics of an asymmetrical rotor-shaft system under a constant driving torque[56,57]. There described how large driving torque is needed to pass the critical speed and what happens when the driving torque is smaller than the minimum torque for passing through the critical speed by using equations of motion based on those obtained in chapter 2.

Chapter 4 analyses the torsional vibration of symmetrical rotor-shaft system[46,47]. The rotating speed where torsional vibration occurs, how large vibration changes as damping coefficients change, and the mechanism how the torsional vibration occurs are described.

Chapter 5 is intended for an asymmetrical rotor-shaft, and its torsional vibration is investigated[58,59]. Asymptotic solutions are also proposed. In addition to the case described in chapter 4, the asymmetry of rotor makes the problem of torsional vibration more difficult.

Our analytical assumption in chapter 2 to 5 are as follows:

(1) Rotor is rigid;

(2) Rotating shaft is elastic and its spring constant for restoring force is linear;
(3) Deformations of rotating shaft (deflection, angle of deflection, and angle of torsion) are small;
(4) No distributed mass is in rotating shaft;
(5) Gravity is ignored.

Chapter 2. Equations of Motion of a Rotor-Shaft System with Variable Rotating Speed[38]

2.1 *Introduction*

Rotating machinery sometimes changes in its shaft speed for some reason such as the starting or stopping of a machine, the operating under a changing load torque, and the driving through a universal joint[32]. The research papers previously in issue, however, do not regularly exhibit equations of motion for such shaft-rotor system. These research papers are divided in terms of equations of motion for a shaft with variable rotating speed, being accompanied by the terms due to the change of rotational speed. This principal difference seems to appear in inertia terms according to whether the equations of motion are derived from Lagrangian formulations[28,39] or Eulerian formulations[22,35,36]. The inertia terms may be expressed as

$$M_r = I\ddot{\theta}_{rz} - iI_p\dot{\Theta}_r\dot{\theta}_{rz} - iI_p\ddot{\Theta}_r\theta_{rz} \tag{2.1}$$

and

$$M_r = I\ddot{\theta}_{rz} - iI_p\dot{\Theta}_r\dot{\theta}_{rz} - \frac{1}{2}iI_p\ddot{\Theta}_r\theta_{rz} \tag{2.2}$$

where I_p is the polar moment of inertia, I the diametral moment of inertia about an axis perpendicular to the polar axis, Θ_r the rotational angle, $\theta_{rz} = \theta_{rx} + i\theta_{ry}$ $(i = \sqrt{-1})$ the inclination angle of the polar axis from the z-axis, projections of which to the xz- and yz-planes are θ_{rx} and θ_{ry} (refer to Fig. 2.2). Superscript dot notations means differentiation with respect to time t. Equation (2.1) appears to be derived from Euler's equation of motion, and Eq. (2.2) from Lagrange's ones.

As for the rotational motion of a rigid body, Euler's equations of motion must be perfectly equivalent to Lagrange's ones. In the light of the foregoing, why is it that the previous equations of motion are not derived in the same way? This problem relates to the dynamical foundation for the vibration analysis of a rotor-shaft system with variable rotating speed. The difference between Eq. (2.1) and Eq. (2.2) yields in the equations of motion which assure an accuracy to the first-order of the shaft deformation. Therefore, our analytical foundation is to consider that the gyroscopic terms contain the socond-order quantities of the shaft deformation. The equations of motion in the present study have an accuracy to the second-order, and explain the appearence of the second-order terms. Because Lagranian in this case requires the deformation energy to the third order, the deformation energy of the shaft to be expressed with an accuracy to the third-order, the deformation energy is derived by applying the theory of elasticity[37] to bending and torsion.

2.2 *Rotor-shaft system*

Consider a rotor-shaft system such as detailed in Fig. 2.1. A rotor D with mass m is mounted on the end S of an overhung shaft S_h.The shaft S_h has a uniform circular section and

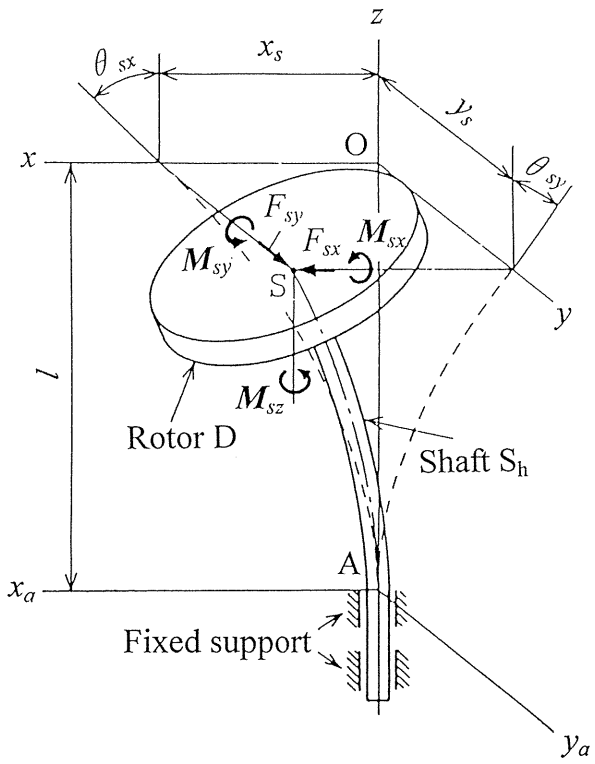

Fig. 2. 1. Rotor-shaft system.

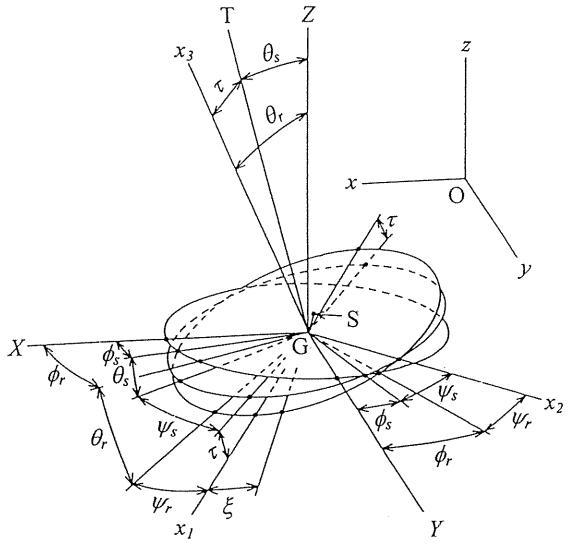

Fig. 2. 2. Coordinate system.

l in length, and is driven at the shaft end A. The driving torque at A-end will change the rotating speed of the shaft.The distributed mass of the shaft and the effect of gravity are neglected. A rectangular coordinate system O-xyz is stationary, and its z-axis coincides with the center line of two ball bearings. The shaft end S is located at the origin O when the shaft is not deformed.

In Fig. 2.2, G-XYZ is a movable rectangular coordinate system parallel to O-xyz, and its origin G is the center of gravity of the rotor D. The axes x_1, x_2, and x_3 fixed on the rotor D are the principal axes of inertia. The x_3-axis, the polar axis, is inclined by τ from the straight line GT parallel to the tangent of the deflection curve at the point S. The azimuth direction of this dynamic unbalance τ is assumed to coincide with the x_1-axis. The center of gravity G is in deviating by e from the point S, and its direction is in advance by β to the sence of shaft rotation from the x_1-axis. Let I be the moment of inertia about the x_1- and x_2-axes, and I_p be the polar moment of inertia about the x_3-axis. Each orientation of the three principal axes of inertia is specified by Eulerian angles θ_r, ϕ_r, and ψ_r, and the orientation of the principal axes of flexible shaft by θ_s, ϕ_s, and ψ_s.

Let the non-dimensional eccentricity e/l and the dynamic unbalance τ be quantities of the same order as the deflection, the angle of deflection, and the angle of torsion. Thus the equations of motion in this paper are derived with an accuracy to the second-order of these small quantities.

2.3 *Lagrange's equations of motion*

2.3.1 *Kinetic energy*

For the kinetic energy of the rotor we have the following expression:

$$T=\frac{1}{2}m(\dot{x}_r^2+\dot{y}_r^2)+\frac{1}{2}I(\omega_1^2+\omega_2^2)+\frac{1}{2}I_p\omega_3^2, \tag{2.3}$$

in which x_r and y_r are the lateral displacements of the center of gravity G to the x- and y-directions; ω_1, ω_2 and ω_3 are the components of the angular velocity vector of the rotor to the x_1-, x_2-, and x_3-axes, respectively.

Now let the inclination of the x_3-axis from the z-axis be θ_r, and the projections of θ_r to the xz- and yz-planes be θ_{rx} and θ_{ry}, respectively, introducing

$$\Theta_r=\phi_r+\psi_r\,. \tag{2.4}$$

Then Eq. (2.3) becomes

$$T=\frac{1}{2}m(\dot{x}_r^2+\dot{y}_r^2)+\frac{1}{2}I(\dot{\theta}_{rx}^2+\dot{\theta}_{ry}^2)+\frac{1}{2}I_p\{\dot{\Theta}_r(\dot{\theta}_{rx}\theta_{ry}-\dot{\theta}_{ry}\theta_{rx})\} \tag{2.5}$$

which neglects small quantities of the fourth and higher powers of θ_r. Expression (2.5) for the kinetic energy coincides with the well-known results obtained by neglecting small quantities of the third and higher powers of θ_{rx} and θ_{ry}.

2.3.2 *Potential energy*

The driving point A is assumed to be subject to the external forces F_{sx} and F_{sy} and the moments of force M_{sx}, M_{sy}, and M_{sz}, deforming the flexible shaft from rotation, as shown in Fig. 2.1. The flexible shaft will undergo deformations of bending and torsion. Under these

conditions the potential energy (i.e., the strain energy stored in the shaft) is produced. Let the bending rigidty of the shaft be EI_0 and the torsional rigidty GI_z. A coordinate s with the driving point A at its origin, is chosen along the center line of the flexible shaft. Then we have the following expression for the potential energy:

$$V=\frac{1}{2}\int_0^l \{EI_0\,(\Omega_\xi^2+\Omega_\eta^2\}ds \tag{2.6}$$

with

$$\left.\begin{aligned}\Omega_\xi &= -\left(\frac{d\theta}{ds}\sin\psi-\frac{d\phi}{ds}\sin\theta\cos\psi\right),\\ \Omega_\eta &= -\left(\frac{d\theta}{ds}\cos\psi+\frac{d\phi}{ds}\sin\theta\sin\psi\right),\\ \Omega_\zeta &= -\left(\frac{d\phi}{ds}\cos\theta+\frac{d\psi}{ds},\right)\end{aligned}\right\} \tag{2.7}$$

in which θ, ϕ, and ψ are Eulerian angles representing the angular positions of the principal axes of the flexible shaft[37]. It is assumed that the three principal axes do not change in these directions along the longitudinal direction of the shaft without deformation.

In Fig. 2.1, let M_ξ, M_η, and M_ζ denote the moments of force acting from the section under a certain point s to that over, in the principal axes of the flexible shaft. Then

$$\left.\begin{aligned}M_\xi &= EI_0\Omega_\xi,\\ M_\eta &= EI_0\Omega_\eta,\\ M_\zeta &= GI_z\Omega_\zeta\end{aligned}\right\} \tag{2.8}$$

hold.

The torsional angle θ_t at a point apart by s from the point A can be defined by

$$\theta_t=\phi+\psi-\Theta_a\,, \tag{2.9}$$

in which Θ_a is the rotational angle at the driving point A. Let the projective angles of θ to the xz- and yz-planes be θ_x and θ_y. Rewriting Eq. (2.6) with an accuracy to the third-order of θ_x, θ_y, and θ_t, we obtain

$$\begin{aligned}V=\frac{1}{2}\int_{-l}^{0}\Bigg[\, EI_0\left\{\left(\frac{d\theta_x}{dz}\right)^2+\left(\frac{d\theta_y}{dz}\right)^2\right\}\\ +GI_z\left\{\left(\frac{d\theta_t}{dz}\right)^2-\frac{d\theta_t}{dz}\left(\theta_x\frac{d\theta_y}{dz}-\theta_y\frac{d\theta_x}{dz}\right)\right\}\Bigg]\,dz,\end{aligned} \tag{2.10}$$

provided that the origin of the z-axis is the point A.

Integrating Eq. (2.8) with Eqs. (2.7) and (2.9) under the boundary condition of Fig. 2.1 gives the angles of deflection $\theta_x(z)$ and $\theta_y(z)$, the angle of torsion $\theta_t(z)$, and the deflections

$x(z)$ and $y(z)$ required to calculate Eq. (2.10). Using these results we derive the deflections x_s and y_s, the angles of deflection θ_{sx} and θ_{sy}, and the angle of torsion θ_{st} at point S:

$$\left.\begin{aligned} &x_s = x(0),\ y_s = y(0), \\ &\theta_{sx} = \theta_x(0),\ \theta_{sy} = \theta_y(0),\ \theta_t = \theta_t(0). \end{aligned}\right\} \tag{2.11}$$

The right-hand side of Eq. (2.11) contains the quantities F_{sx}, F_{sy}, M_{sx}, M_{sy}, and M_{sz}. Accordingly, solving Eq. (2.11) for these quantities yields

$$\left.\begin{aligned} F_s &= \alpha z_s + \gamma\theta_{sz} + i\frac{\delta_t}{l}\theta_{st}\theta_{sz}, \\ M_s &= \gamma z_s + \delta\theta_{sz} - i\delta_t\theta_{st}\left(\frac{\theta_{sz}}{2} + \frac{z_s}{l}\right), \\ M_{sz} &= \delta_t\theta_{st} - \left(\gamma + \frac{\delta_t}{l}\right)(x_s\theta_{sy} - y_s\theta_{sx}) \end{aligned}\right\} \tag{2.12}$$

with the spring constants

$$\alpha = \frac{12EI_0}{l^3},\ \gamma = -\frac{6EI_0}{l^2},\ \delta = \frac{4EI_0}{l},\ \delta_t = \frac{GI_z}{l} \tag{2.13}$$

and the complex numbers

$$\left.\begin{aligned} F_s &= F_{sx} + iF_{sy}, \\ M_s &= M_{sy} - iM_{sx}, \\ z_s &= x_s + iy_s, \\ \theta_{sz} &= \theta_{sx} + i\theta_{sy}. \end{aligned}\right\} \tag{2.14}$$

Now we can carry out integration of Eq. (2.10) with an accuracy to the third powers of θ_{sx}, θ_{sy}, θ_{st}, x_s/l, and y_s/l, find our way to the following expression for the potential energy:

$$V = \frac{1}{2}\alpha(x_s^2 + y_s^2) + \gamma(x_s\theta_{sx} + y_s\theta_{sy}) + \frac{1}{2}\delta(\theta_{sx}^2 + \theta_{sy}^2) + \frac{1}{2}\delta_t\theta_{st}^2 \underline{- \frac{\delta_t}{l}\theta_{st}(x_s\theta_{sy} - y_s\theta_{sx})}. \tag{2.15}$$

The appearance of Eq. (2.15) differs from that of the potential energy presented previously in that Eq. (2.15) contains the underlined small term of the third-order. Previous expressions for the potential energy[7,39] show $-M_{az}\Theta_s$ (based on the notation of this paper) in place of the fourth term $(1/2)\delta_t\theta_{st}^2$ in the right-hand side of Eq. (2.15), where M_{az} represents the driving torque. Such term produces in the potentional energy the work the constant driving torque M_{az} performs while the shaft rotates by Θ_s. Only for the rigid shaft is this consideration possible. The expression $-M_{az}\Theta_s$ in the potential energy is necessary to consider the change of the driving torque $-M_{az}$ proportional to the torsional angle θ_{st} from zero to a certain value.

2.3.3 *Dissipation function*

Assume that the rotor is subjected to viscous friction for the translation and the rotational motion about the axis perpendicular to the polar axis, and about the polar axis, whose damping coefficients are c_1, c_2, and c_3, respectively. Then the dissipation function F is obtained by putting c_1, c_2, and c_3 in place of m, I, and I_p in Eq. (2.3).

$$F=\frac{1}{2}c_1(\dot{x}_r^2+\dot{y}_r^2)+\frac{1}{2}c_2(\omega_1^2+\omega_2^2)+\frac{1}{2}c_3\omega_3^2 \tag{2.16}$$

2.3.4 *Lagrange's Equations of motion*

Between the rotational angle Θ_r of the rotor and that Θ_s of the shaft, we find the relation:

$$\Theta_r=\Theta_s+\frac{\tau}{2}(\theta_{sx}\sin\Theta_s-\theta_{sy}\cos\Theta_s). \tag{2.17}$$

Now we introduce the following complex numbers:

$$\left.\begin{aligned} z_r&=x_r+iy_r=z_s+e\exp\{i(\Theta_s+\xi)\},\\ \theta_{rz}&=\theta_{rx}+i\theta_{ry}=\theta_{sz}+\tau\exp(i\Theta_s).\end{aligned}\right\} \tag{2.18}$$

Considering Eqs. (2.17) and (2.18), and substituting Eqs. (2.5), (2.15), and (2.16) along with the dissipation function F into Lagrange's equations of motion, we obtain the following equations of motion:

$$M_I-\frac{1}{2}i(I_p\ddot{\Theta}_s+c_3\dot{\Theta}_s-\delta_t\theta_{st})\,\theta_{sz}=0, \tag{2.19}$$

$$M_R-me\{\ddot{x}_s\sin(\Theta_s+\xi)-\ddot{y}_s\cos(\Theta_s+\xi)\}=0, \tag{2.20}$$

$$\begin{aligned} &m\ddot{z}_s+c_1\dot{z}_s+F_s\\ &\quad=me\dot{\Theta}_s^2\exp\{i(\Theta_s+\xi)\}-ie(m\ddot{\Theta}_s+c_1\dot{\Theta}_s)\exp\{i(\Theta_s+\xi)\},\end{aligned} \tag{2.21}$$

where

$$\begin{aligned} M_I&=I\ddot{\Theta}_{sz}-iI_p\dot{\Theta}_s\dot{\theta}_{sz}+c_2\dot{\theta}_{sz}+M_s\\ &\quad-\tau(I-I_p)\,\dot{\Theta}_s^2\exp(i\Theta_s)+i\tau\{(I-I_p)\,\ddot{\Theta}_s+(c_2-c_3)\,\dot{\Theta}_s)\exp\{i(\Theta_s)\},\end{aligned} \tag{2.22}$$

$$\begin{aligned} M_R&=I_p\ddot{\Theta}_s+c_3\dot{\Theta}_s+\delta_t\theta_{st}-\frac{\delta_t}{l}(x_s\theta_{sy}-y_s\theta_{sx})\\ &\quad+\frac{1}{2}I_p(\ddot{\theta}_{sx}\theta_{sy}-\ddot{\theta}_{sy}\theta_{sx})-\tau(I-I_p)(\ddot{\theta}_{sx}\sin\Theta_s-\ddot{\theta}_{sy}\cos\Theta_s).\end{aligned} \tag{2.23}$$

The driving torque M_{az} at the point A is defined from the equilibrium equation for the moment of force:

$$M_{az} = -\delta_t \theta_{st} + \frac{\delta_t}{l}(x_s \theta_{sy} - y_s \theta_{sx}). \tag{2.24}$$

2.4 *Euler's equations of motion*

Neglecting small quantities of the third and higher powers of θ_r, we can express Euler's equations of motion by the following forms:

$$\left.\begin{aligned} &H_x \cos \Theta_r + H_y \sin \Theta_r = K_1 - c_1 \omega_1, \\ &H_y \cos \Theta_r - H_x \sin \Theta_r = K_2 - c_2 \omega_2, \\ &I_p \ddot{\Theta}_r + \frac{1}{2} I_p (\ddot{\theta}_{rx} \theta_{ry} - \ddot{\theta}_{ry} \theta_{rx}) = K_3 - c_3 \omega_3, \end{aligned}\right\} \tag{2.25}$$

where

$$\left.\begin{aligned} H_x &= I_p \dot{\Theta}_r \dot{\theta}_{rx} - I \ddot{\theta}_{ry}, \\ H_y &= I_p \dot{\Theta}_r \dot{\theta}_{ry} - I \ddot{\theta}_{rx}. \end{aligned}\right\} \tag{2.26}$$

The notation for K_1, K_2, and K_3 in Eq. (2.25) represents the components to the x_1-, x_2-, and x_3-axes of the moment of restoring force about the center of gravity G, respectively.

We assumed in advance that the deflections x_s and y_s, the angles of deflection θ_{sx} and θ_{sy}, and the angle of torsion θ_{st} were caused at the point S of the shaft under the action of the forces F_{sx} and F_{sy}, and the moments of force M_{sx}, M_{sy}, and M_{sz} on the point S. Therefore, if the deflections, the angles of deflection, and the angle of torsion at the point S are x_s, y_s, θ_{sx}, θ_{sy}, and θ_{st}, then the restoring force and the moments of restoring force must be $-F_{sx}$, $-F_{sy}$, $-M_{sx}$, $-M_{sy}$, and $-M_{sz}$. On these basis of this consideration K_1, K_2, and K_3 are given by

$$\left.\begin{aligned} K_1 &= -(M_{sx} - \theta_{rx} M_{sz}) \cos \Theta_r - (M_{sy} - \theta_{ry} M_{sz}) \sin \Theta_r, \\ K_2 &= (M_{sx} - \theta_{rx} M_{sz}) \sin \Theta_r - (M_{sy} - \theta_{ry} M_{sz}) \cos \Theta_r, \\ K_3 &= -\theta_{rx} M_{sx} - \theta_{ry} M_{sy} - M_{sz} + M_e, \end{aligned}\right\} \tag{2.27}$$

in which

$$M_e = e(\alpha y_s + \gamma \theta_{sy}) \cos(\Theta_r + \xi) - e(\alpha x_s + \gamma \theta_{sx}) \sin(\Theta_r + \xi). \tag{2.28}$$

Equation (2.25) expresses the equilibrium for the moments of force in the principal axes of inertia, is rewritten into the equilibrium equations to the x-, y-, and z-axes by using the direction cosines of the principal axes of inertia. Substitution of Eqs. (2.12), (2.17), (2.19), and (2.27) into Eq. (2.25) leads to the following equations for the inclinational and rotational motions at the point S of the rotating shaft:

$$M_I - i(I_p \ddot{\Theta}_s + c_3 \dot{\Theta}_s)\, \theta_{sz} = 0 \tag{2.29}$$

$$M_R + \theta_{sx}(I\ddot{\theta}_{sy} - I_p\dot{\Theta}_s\dot{\theta}_{sx} + \gamma y_s) - \theta_{sy}(I\ddot{\theta}_{sx} + I_p\dot{\Theta}_s\dot{\theta}_{sy} + \gamma x_s)$$
$$-M_e - \tau\dot{\Theta}_s^2(I - I_p)(\theta_{sx}\sin\Theta_s - \theta_{sy}\cos\Theta_s) = 0. \tag{2.30}$$

The translation of the rotor is given by Newton's law of motion:

$$m\ddot{z}_r = -F_s - c_1\dot{z}_r, \tag{2.31}$$

which becomes the same expression as Eq. (2.21) by using z_s in place of z_r.

2.5 *Comparison of Lagrange's and Euler's equations of motion*

Equations (2.19) and (2.20) from Lagrange's equation of motion do not coincide in appearance with the corresponding Eqs. (2.29) and (2.30) from Euler's equations. Referring to Eq. (2.20), we find the relation

$$\delta_t\theta_{st}\theta_{sz} = -(I_p\ddot{\Theta}_s + c_3\dot{\Theta}_s)\,\theta_{sz}, \tag{2.32}$$

by which Eq. (2.19) becomes Eq. (2.29) with an accuracy of the second-order. Similarly, Eq. (2.20) becomes Eq. (2.30) by using Eqs. (2.19) and (2.21).

Thus Eqs. (2.19) and (2.20) are equvalent to Eqs. (2.29) and (2.30), respectively. Euler's equations of motion show the projections of the changes in angular momentum per unit time and the moments of force to the rectanguler coordinate axes x, y, and z, while Lagrange's equation show these projections to the directions of $\dot{\theta}_{sx}$(y-direction), $\dot{\theta}_{sy}$($-x$-directions), and $\dot{\Theta}_s = \dot{\phi}_s + \dot{\psi}_s$. Further, the $\dot{\Theta}_s$-direction is defined by the resultant vector of the vector $\dot{\phi}_s$ in the z-direction and the vector $\dot{\psi}_s$ in the tangent (GT-direction in Fig. 2.2) at the point S of the deflection curve. The $\dot{\Theta}_s$-direction is perpendicular neither to the $\dot{\theta}_{sx}$-direction nor $\dot{\theta}_{sy}$-direction.

2.6 *Conclusions*

(1) Applying Lagrange's equations of motion for the shaft with variable rotating speed derives the expressions different in appearance from the result by applying Euler's equations of motion, but they are essentially equivalent.

(2) It is due to lacking an accuracy of the second-order quantities of the shaft deformation that previous equations of motion do not necessarily coincide.

(3) When the kinetic energy and the potentional energy are considered with an accuracy to the third-order of the deflections, the angles of deflection, and the angle of torsion, the kinetic energy is given by Eq. (2.5), which coincides with the previous result assuring an accuracy to the second-order. The potential energy, however, is given by Eq. (2.15), which is not presented in the previous papers.

Chapter 3. Passing through the Critical Speed of an Asymmetrical Rotor-Shaft System under Constant Driving Torque[56,57]

3.1 *Introduction*

In a rotating shaft system with an asymmetrical rotor[61], there is an unstable region where the shaft deflection may increase infinitely. Therefore, it may be more difficult for the system to pass through the critical speed in an asymmetrical system than that in a symmetrical one. Many studies on the critical speed passing problem have been made. But there are few studies on a symmetrical shaft with an asymmetrical rotor[13)-19)], and there are some studies on an asymmetrical shaft with a symmetrical rotor[10)-12)].

This chapter deals with a system consisting of a symmetrical shaft and an asymmetrical rotor. The purpose is to know characteristics about the whirling and the rotating speed of a shaft passing through its critical speed with a constant driving torque. Under the constant driving torque, the rotating speed will be related to the whirling amplitude of shaft. How much is the driving torque enough to pass smoothly through the critical speed or the unstable region? In order to analyse this problem, the present equations of motion have an accuracy of the second-order quantities for the deflection, the angle of deflection, and the torsion. Then the equations of motion are reduced to approximate equations by using the asymptotic method[45]. These analytical results explain how the amplitude and the rotating speed change.

3.2 *Rotor-shaft system and equations of motion*

3.2.1 *Rotor-shaft system and coordinates*

Consider a rotor-shaft system such as detailed in Fig. 3.1. An asymmetrical rotor D with mass m is mounted on the end S of an overhang flexible shaft S_h. The shaft S_h has a uniform circular section and l in length, and is driven at the shaft end A. The driving torque T, at the A-end will change the rotating speed. The A-end and the point S rotate with angular velocities ω_a and ω, and their rotational angles are assumed to be Θ_a and Θ, respectively. Thereby hold $\omega_a = \dot{\Theta}_a$ and $\omega = \dot{\Theta}$, where the superscript dot notation means differentiation with respect to time t. The distributed mass of the shaft S_h and the effect of gravity are neglected. A rectangular coordinate system O-xyz is stationary, and its z-axis coincides with the center line of two ball bearings. The shaft end S is located at the origin O when the shaft is not deformed.

In Fig. 3.2, G-XYZ is a movable rectangular coordinate system parallel to O-xyz, and its origin G is the center of gravity of the rotor D. The axes x_1, x_2, and x_3 fixed on the rotor D are the principal axes of inertia; the x_3-axis, the polar axis, is inclined by τ from the straight line GT parallel to tangent of the deflection curve at the point S. The azimuth direction of this dynamic unbalance τ is in advance by η to the sense of shaft rotation from the x_1-axis. The center of gravity G, furthermore, is in deviating by e from the point S, and its direction is in advance by ξ to the sense of shaft rotation from the x_1-axis. The moments of inertia about the x_1-, x_2-, and x_3-axes are I_1, I_2 ($I_1 > I_2$), and I_3, respectively.

When the flexible shaft has some deformations, the point S deviates by x, y in the x-, y-directions, and the tangent of the deflection curve at the point S is θ. Let θ_x and θ_y be the projections of θ to the xz- and yz-planes, respectively. The torsional angle of shaft is defined as the difference between the rotational angle Θ_a at the point A and that Θ at the point S:

$$\theta_t = \Theta - \Theta_a . \tag{3.1}$$

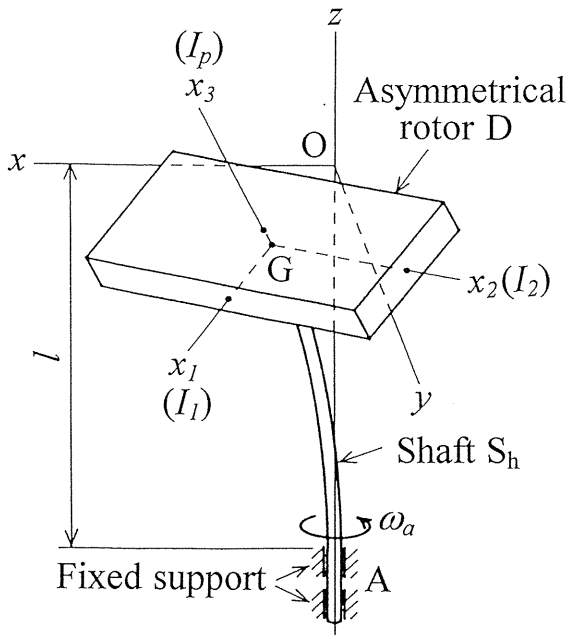

Fig. 3. 1. Asymmetrical rotor-shaft system.

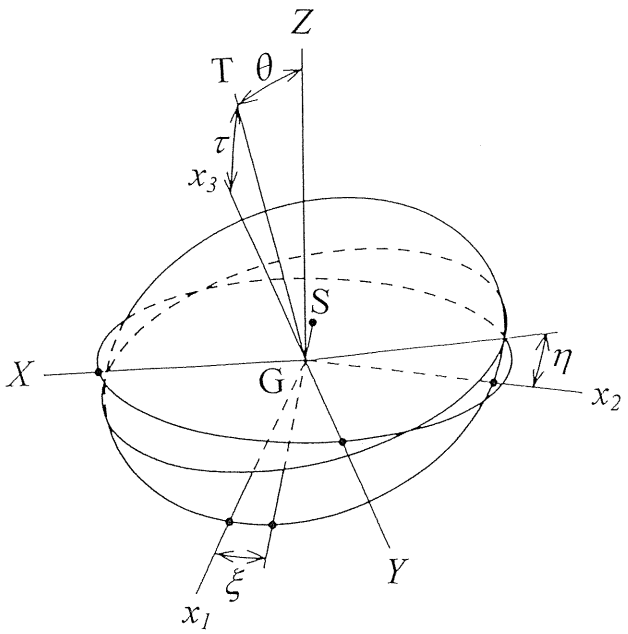

Fig. 3. 2. Relative angular positions ξ and η of eccentricity $\overline{GS} = e$ and dynamic unbalance τ to principal axes of inertia x_1, x_2, and x_3.

We assume that the non-dimensional eccentricity e/l and the dynamic unbalance τ are small quantities of the same order as the deflection, the angle of deflection, and the angle of torsion. Thus, the equations of motion in this chapter are derived with an accuracy to the second-order of these small quantities. Now we introduce the following complex numbers:

$$z = \frac{x}{l} + i\frac{y}{l}, \quad \theta_z = \theta_x + i\theta_y, \tag{3.2}$$

in which $i = \sqrt{-1}$.

Let α, γ, and δ be the spring constants for lateral displacements of the shaft, δ_t be the spring constant for torsion of the shaft, and c_1, c_2, and c_3 be the damping coefficients for translation, inclination, and rotation of the rotor, respectively.

3.2.2 *Equations of motion*

Here we introduce the following non-dimensional parameters:

$$\left.\begin{aligned}
&e' = e/l,\ T_r' = T_r/(\alpha l^2),\ \gamma' = \gamma/(\alpha l),\ \delta' = \delta/(\alpha l^2),\ \delta_t' = \delta_t/(\alpha l^2),\\
&c_1' = c_1/\sqrt{m\alpha},\ c_2' = c_2/(l^2\sqrt{m\alpha}),\ c_3' = c_3/(l^2\sqrt{m\alpha}),\\
&\omega_a' = \omega_a/\sqrt{\alpha/m},\ \omega' = \omega/\sqrt{\alpha/m},\ t' = t\sqrt{\alpha/m},\\
&I = (I_1 + I_2)/(2ml^2),\ I_p' = I_p/(ml^2),\ \Delta I = (I_1 - I_2)/(2ml^2).
\end{aligned}\right\} \tag{3.3}$$

Hereafter, the primes in Eq. (3.3) are omitted.

The kinetic energy of the rotor is given as the sum of the energy for translation and that for rotational motion. The potential energy of the flexible shaft is derived by using theory of elasticity to bending and torsion[37]. The dissipation function is calculated under the assumption that the rotor is subjeted to viscous frictions for the translation, the rotational motion about the polar axis, and that about the axis perpendicular to the polar axis. Substituting the kinetic energy, the potential energy, and the dissipation function into Lagrange's equations of motion, we obtain the following equations of motion:

$$\ddot{z} + z + \gamma\theta_z = -c_1\dot{z} - i\delta_t\theta_t\theta_z + e\left\{\dot{\Theta}^2 - i(\ddot{\Theta} + c_1\dot{\Theta})\right\}\exp\{i(\Theta + \xi)\}, \tag{3.4}$$

$$\begin{aligned}
I\ddot{\theta}_z - iI_p\dot{\Theta}\dot{\theta}_z + \delta\theta_z + \gamma z = {} & -c_2\dot{\theta}_z + i\delta_t\theta_t z + \frac{i\theta_z}{2}(I_p\ddot{\Theta} + c_3\dot{\Theta})\\
& + \tau\left[(I - I_p)\dot{\Theta}^2 - i\left\{(I - I_p)\ddot{\Theta} + (c_2 - c_3)\dot{\Theta}\right\}\right]\exp\{i(\Theta + \eta)\}\\
& + \Delta I\frac{d}{dt}\left[\dot{\bar{\theta}}_z\exp\{2i\Theta\} - i\tau\dot{\Theta}\exp\{i(\Theta - \eta)\}\right],
\end{aligned} \tag{3.5}$$

$$\begin{aligned}
I_p\ddot{\Theta} + c_3\dot{\Theta} = {} & T_r + \mathrm{Im}\left[\frac{1}{2}I_p\ddot{\theta}_z\bar{\theta}_z - \left\{\Delta I\dot{\theta}_z^2\exp(-i\Theta) + \tau\Delta I\ddot{\theta}_z\exp(i\eta)\right.\right.\\
& \left.\left. + e\ddot{z}\exp(-i\xi) + \tau(I - I_p)\ddot{\theta}_z\exp(-i\eta)\right\}\exp(-i\Theta)\right],
\end{aligned} \tag{3.6}$$

where $\bar{\theta}_z$ is a conjugate complex number of θ_z, Im[ ] represents an imaginary part in [ ], and the superscript dot notation means differentiation with respect to non-dimensional time t. The torsional angle θ_t is given by the following equation:

$$\theta_t = -\mathrm{Im}[z\bar{\theta}_z] - \frac{T_r}{\delta_t}. \tag{3.7}$$

As the driving torque T_r is given as a constant value, substituting Eq. (3.7) into Eqs. (3.4) and (3.5) and integrating Eqs. (3.4), (3.5), and (3.6) give z, θ_z, and Θ. The rotational angle Θ_a at the driving point is

$$\Theta_a = \Theta - \theta_t. \tag{3.8}$$

The rotating shaft system has four natural angular frequencies for the whirling vibrations. Let these frequencies be p_1, p_2, p_3, and p_4 in order of size. We deal with the case that the shaft system is going to pass through the critical speed $\omega = p_2$ under the constant driving torque T_r. The rotating speed does not always change smoothly because of the finite driving torque. The asymptotic method is now applied to analyse the nonlinear equations of motion (3.4), (3.5), and (3.6). The rotating shaft is assumed to vibrate with single whirling mode of frequency p_2. Under the above assumption, we can construct the asymptotic equations[45] for the equations of motion. The first approximate equations are as follows:

$$z = A_2 \exp\{i(\Theta + \Phi_2)\}, \quad \theta_z = \kappa_2 A_2 \exp\{i(\Theta + \Phi_2)\}, \tag{3.9}$$

$$\left.\begin{aligned} \dot{A}_2 &= -\zeta_2 A_2 + e\mu_2 \sin(\Phi_2 - \xi) + \tau\nu_2 \sin(\Phi_2 - \eta) + \Delta I\sigma_2 A_2 \sin 2\Phi_2, \\ \dot{\Phi}_2 &= p_2 - \omega + \frac{e\mu_2}{A_2}\cos(\Phi_2 - \xi) + \frac{\tau\nu_2}{A_2}\cos(\Phi_2 - \eta) + \Delta I\sigma_2 \cos 2\Phi_2, \end{aligned}\right\} \tag{3.10}$$

where

$$\kappa_2 = -(1 - p_2^2)/\gamma, \tag{3.11}$$

$$\zeta_2 = \frac{2(c_1 + c_2\kappa_2^2)p_2 - T_r\kappa_2^2 + D_2\dot{\omega}}{2\kappa_2^2(2Ip_2 - I_p\omega) + 4p_2}, \tag{3.12}$$

$$\left.\begin{aligned} \mu_2 &= -\frac{\omega^2}{\kappa_2^2\{I(p_2 + \omega) - I_p\omega\} + p_2 + \omega}, \\ \nu_2 &= -\frac{(I - I_p)\kappa_2\omega^2}{\kappa_2^2\{I(p_2 + \omega) - I_p\omega\} + p_2 + \omega}, \end{aligned}\right\} \tag{3.13}$$

$$\sigma_2 = -\frac{\kappa_2^2 p_2(2\omega - p_2)}{\omega\{2 + (2I - I_p)\kappa_2^2\}}, \tag{3.14}$$

$$D_2 = 2(1 + I\kappa_2^2)\frac{dp_2}{d\omega} + 2(2Ip_2 - I_p\omega)\kappa_2\frac{d\kappa_2}{d\omega}. \tag{3.15}$$

Substitution of Eq. (3.9) with Eq. (3.10) into Eq. (3.6) derives the following equation:

$$\begin{aligned} I_p\dot{\omega} + c_3\omega &= T_r + \Delta I\kappa_2{}^2 p_2{}^2 A_2{}^2 \sin 2\Phi_2 + \tau\Delta I\kappa_2 p_2{}^2 A_2 \sin(\Phi_2 + \eta) \\ &+ ep_2{}^2 A_2 \sin(\Phi_2 - \xi) + \tau(I - I_p)\kappa_2 p_2{}^2 A_2 \sin(\Phi_2 - \eta)\,, \end{aligned} \tag{3.16}$$

which determines the angular velocity ω. In this case $\omega_a = \omega$ holds by Eqs. (3.7) ~ (3.9).

3.3 *Numerical results*

The approximate equations will be useful for expressing numerically the whirling amplitude and the rotating speed, etc. We use the following parameters to obtain the numerical results:

$$\left.\begin{aligned} &I = 0.0534, \quad I_p = 0.1034, \\ &\delta = 1/3, \quad \delta_t = 0.0655, \quad \gamma = -0.5, \quad c_3 = 1.0 \times 10^{-4}. \end{aligned}\right\} \tag{3.17}$$

The remaining parameters are shown in each calculation. All initial values in case of numerical integration take the solution in steady state.

3.3.1 *Unstable region*

Analysing Eq. (3.10) for constant ω gives the condition whether the rotating shaft system is stable or not. Figure 3.3 shows the unstable region, which expands around $\omega = 0.53$ as the asymmetry $\Delta I/I$ increases. Furthermore, this value 0.53 is nearly equal to the critical speed ω_c when $\Delta I = 0$.

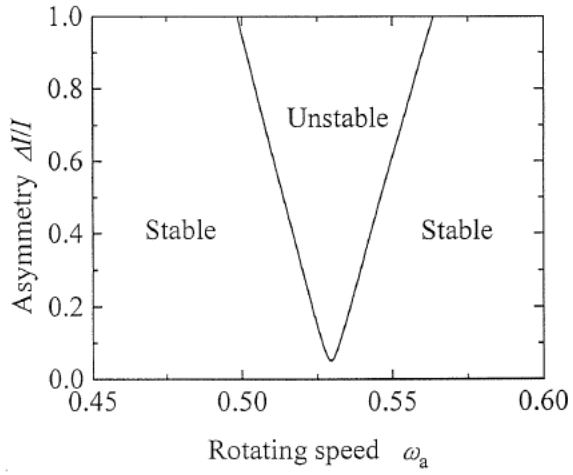

Fig. 3. 3. Unstable region ($c_1 = c_2 = 1.0 \times 10^{-3}$).

3.3.2 *General vibration characteristics of asymmetrical rotor*

(i) Case of comparatively large driving torque

Figures 3.4(a) and 3.4(b) demonstrate the amplitude A_2 and the rotating speed ω obtained by integrating Eqs. (3.10) and (3.16). The unstable region is about from $\omega = 0.52$ to $\omega = 0.54$, because the asymmetry $\Delta I/I$ is 0.275. The manner by which the amplitude changes is qualitatively similar to the results for a symmetrical rotor[18]. The larger driving torque becomes, the smaller maximum amplitude becomes in passing through the first critical speed.

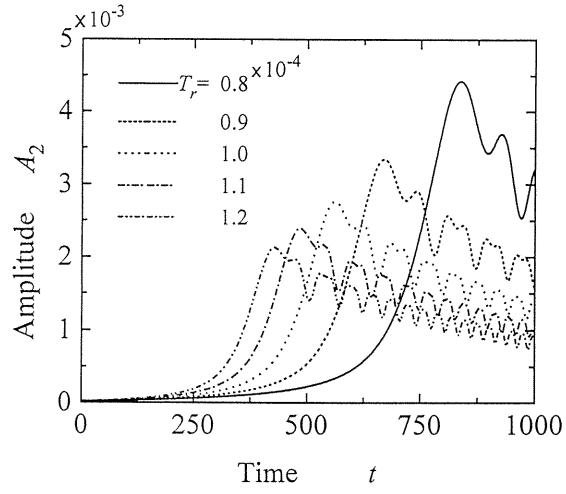

(a) Amplitude response

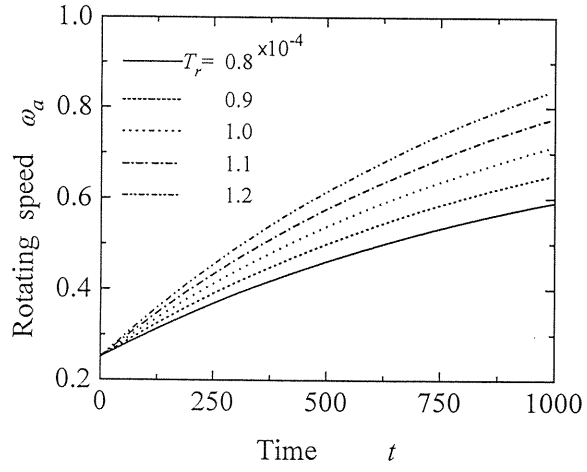

(b) Rotating speed response

Fig. 3. 4. Case of comparatively large driving torque ($\Delta I = 0.0147$, $e = 0.9 \times 10^{-4}$, $\tau = 4.6 \times 10^{-4}$, $\xi = \eta = 0°$, $c_1 = c_2 = 1.0 \times 10^{-3}$).

The rotating speed increases smoothly, and passes easily through the critical speed $\omega_{ac} = 0.53$ and the unstable region. As the driving torque T_r becomes large, the angular acceleration increases. It is caused by the effect of the damping coefficient c_3 that the rotating speed does not increase linearly. Therefore, the rotating speed must finally get the value T_r/c_3, which is obtained by neglecting the second term of the right hand side in Eq. (3.6) and by putting $\dot{\omega} = 0$.

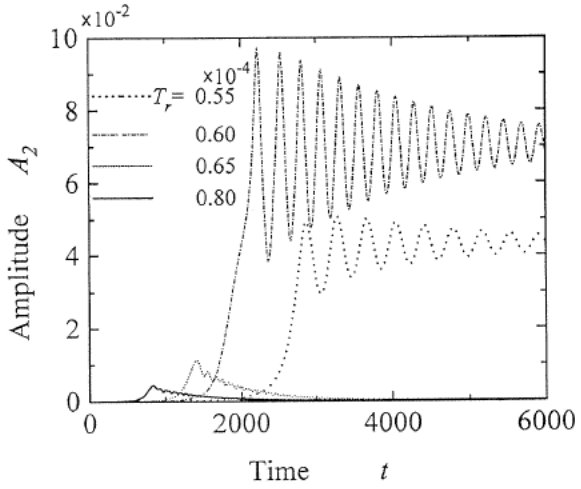

(a) Amplitude response

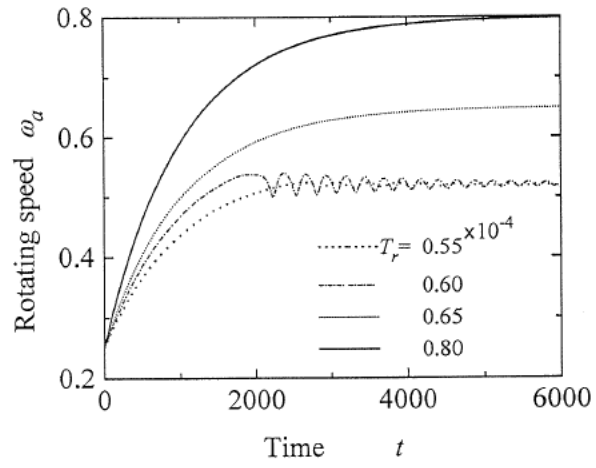

(b) Rotating speed response

Fig. 3. 5. Case of comparatively small driving torque ($\Delta I = 0.0147$, $e = 0.9 \times 10^{-4}$, $\tau = 4.6 \times 10^{-4}$, $\xi = \eta = 0°$, $c_1 = c_2 = 1.0 \times 10^{-3}$).

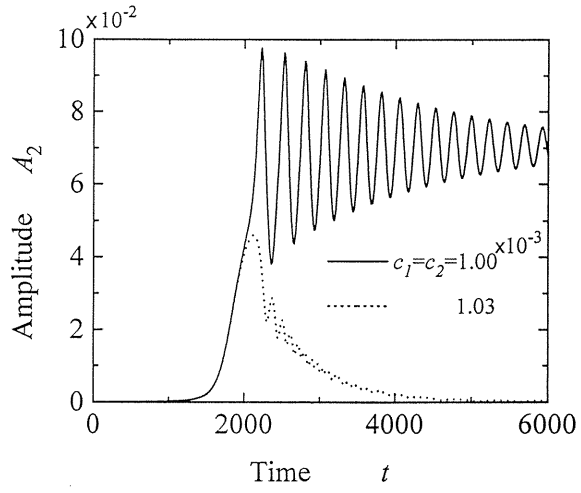

(a) Amplitude response

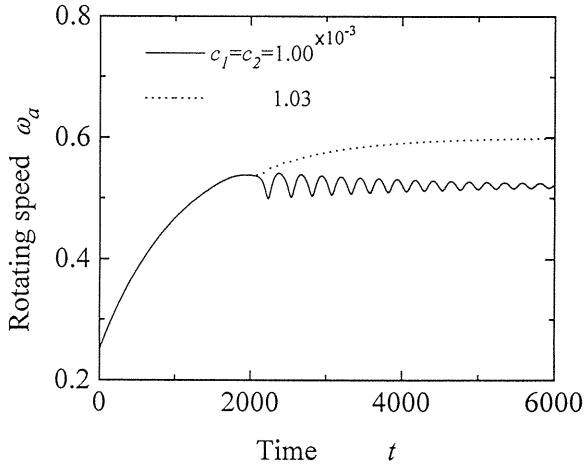

(b) Rotating speed response

Fig. 3. 6. Influence of damping coefficients on amplitude and rotating speed ($T_r = 0.6 \times 10^{-4}$, $\Delta I = 0.0147$, $e = 0.9 \times 10^{-4}$, $\tau = 4.6 \times 10^{-4}$, $\xi = \eta = 0°$).

(ii) Case of comparatively small driving torque

Figures 3.5(a) and 3.5(b) show the results for the driving torques smaller than those in Fig. 3.4. The driving torques $T_r = 0.55 \times 10^{-4}$ and 0.60×10^{-4} are too small to pass through the critical speed, the amplitude A_2 becomes far larger than that in Fig. 3.4. The rotating speed ω, after smooth increase to the neighborhood of the critical speed, fluctuates around the critical speed, to say more precisely, the lower boundary of the unstable region, and never passes the critical speed. After that it seems as if the rotating speed converged the lower

boundary of the unstable region. Similarly, the amplitude A_2 increases smoothly and converges a value while fluctuating. When the driving torque T_r takes 0.80×10^{-4} or 0.65×10^{-4}, the rotating speed approaches gradually $T_r/c_3 = 0.80$ or 0.65. The rotating speed, however, fluctuates about the value smaller than $T_r/c_3 = 0.60$ or 0.55 when the driving torque takes 0.60×10^{-4} or 0.55×10^{-4}. This rotating speed response relates to the energy dissipation in the whirling vibration. Part of the torque is spent to sustain the whirling vibration, the rest is spent to accelerate the rotating speed. The whirling vibration under the driving torque $T_r = 0.60 \times 10^{-4}$ spends the torque $c_3\,(0.60 - 0.52) = 0.8 \times 10^{-5}$, and that under $T_r = 0.55 \times 10^{-4}$ spends the torque 0.3×10^{-5}. So the former amplitude becomes larger than the latter amplitude.

3.3.3 *Effects of damping coefficients for whirling vibrations*

If the damping coefficients for whirling vibrations are made larger, the system might be able to pass through the critical speed even if the driving torque is very small. As shown in Figs. 3.6(a) and 3.6(b), the shaft system when $c_1 = c_2 = 1.00 \times 10^{-3}$ cannot pass the critical speed ω_c. In this case the changes of A_2 and ω are similar to those shown in Figs. 3.5(a) and 3.5(b) for $T_r = 0.60 \times 10^{-4}$. Whereas slightly larger damping coefficients ($c_1 = c_2 = 1.03 \times 10^{-3}$) than 1.00×10^{-3} enable the system to pass it. This slight difference in the damping coefficient about 1.00×10^{-3} affects considerably the behavior of the system.

3.3.4 *Effects of asymmetry and eccentricity*

Figure 3.7 shows the change of the maximum amplitude $A_{2\max}$ to the angular position of eccentricity ξ keeping the relation $\eta = \xi + 180$ degrees. The pattern $A_{2\max}$ to ξ is like a sine-curve. The maximum amplitude takes the maximum value near $\xi = 40$ degrees and 220 degrees, while it takes the minimum value near $\xi = 130$ degrees and 310 degrees. When the maximum amplitude $A_{2\max}$ takes the minimum value, the $A_{2\max}$-value is smaller than that of symmetrical rotor ($\Delta I/I = 0.0$), and the asymmetrical system may pass the critical speed

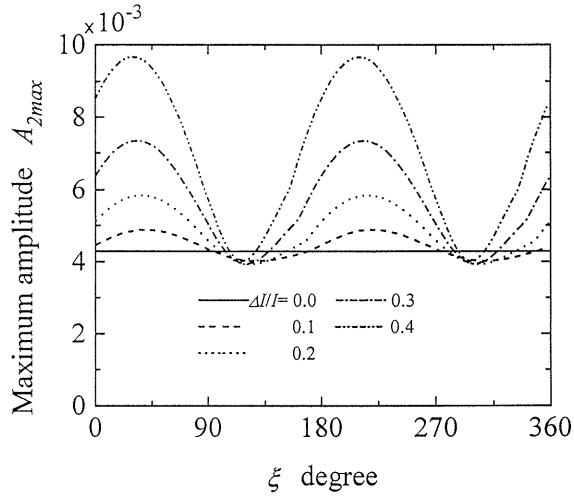

Fig. 3. 7. Influence of asymmetry on maximum amplitude ($T_r = 1.0 \times 10^{-4}$, $e = 0.9 \times 10^{-4}$, $\tau = 4.6 \times 10^{-4}$, $\eta = \xi + 180°$, $c_1 = c_2 = 1.0 \times 10^{-3}$).

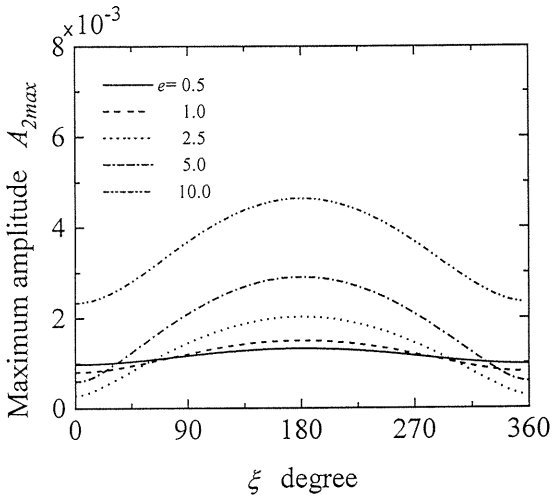

Fig. 3. 8. Influence of eccentricity on maximum amplitude ($T_r = 1.0 \times 10^{-4}$, $\Delta I = 0.0147$, $\tau = 4.6 \times 10^{-4}$, $\eta = 0°$, $c_1 = c_2 = 1.0 \times 10^{-3}$).

more smoothly than symmetrical system. The rotating shaft presents such behaviors because of the effects of asymmetry $\Delta I/I$, eccentricity e, and dynamic unbalance τ canceled each other at those angles.

Figure 3.8 shows the result when only the angular position of eccentricity ξ changes. The maximum amplitude $A_{2\max}$ is very small when $e = 3.5 \times 10^{-5}$ and $\xi = 0$ degree. Consequently, the system balances well by choosing suitably the magnitude and the angular position of eccentricity.

These are similar results to the case caused in constant angular accelaration[18], and the same consideration of dynamics can be made.

3.4 *Conclusions*

(1) A rotating shaft with an asymmetrical rotor needs the minimum limit driving torque to pass through the critical speed. If the driving torque is much larger than the minimum, the shaft system can pass smoothly through the critical speed. If smaller, the rotating speed fluctuates around the critical speed and the amplitude goes up to a high value.

(2) In cases of too small driving torque to pass the critical speed, a little larger damping coefficients for whirling vibrations may enable the system to pass it. When the rotating shaft can pass through the critical speed because of larger damping coefficients, the pattern of amplitude to time is not like that in cases of smaller damping coefficients.

(3) An increase in asymmetry does not always enlarge the maximum amplitude. The magnitude of the maximum amplitude depends also on the angular position and the magnitude of eccentricity.

Chapter 4. Torsional Vibration of a Symmetrical Rotor-Shaft System under Constant Angular Acceleration[46,47]

4.1 *Introduction*

This chapter deals with the torsional vibration of a rotating shaft when it is passing its critical speed of whirling with a constant angular acceleration. In most cases the torsional vibration is noticed in the systems which have gears or universal joints because such elements have causes of the vibration. But the present rotor-shaft system is so simple that it consists of a symmetrical shaft fixedly supported at both ends and a symmetrical rotor attached at the middle of the shaft. This system seems to have no causes for torsional vibration. Chapter 3 shows some possibility of torsional vibration in the system with variable rotating speed.

A rotating shaft in passing its critical speed will experience periodic stress change caused by whirling vibration with different angular frequency from rotating speed. On the other hand, a torsional vibration surely causes periodic stress change and thereby the rotationg shaft exposes itself to danger of fatigue destruction. Therefore, it is very important to analize whether the torsional vibration occurs in passing the critical speed and if it does occur, how large it will be. This study presents that the torsional vibration really occurs even in a simple rotor-shaft system and that its amplitude depends both on angular acceleration and on damping coefficients. And we considered how the torsional vibration occurs.

4.2 *Rotor-shaft system and equations of motion*

4.2.1 *Rotor-shaft system and coordinates*

Consider a rotor-shaft system such as detailed in Fig. 4.1. A symmetrical rotor D with mass m is mounted on a point S of a flexible shaft S_h fixedly supported at both ends A and B. The shaft S_h has a uniform circular section and l in length, and is driven at the shaft end A. The distance from A to S is l_1. Forced acceleration at the driving point A will cause a torsional vibration at the same time as change the average magnitude of rotating speed at the point S. Let T_r be a driving torque at the A-end. The A-end and the point S rotate with angular velocities ω_a and ω, and their rotational angles are assumed to be Θ_a and Θ, respectively. Thereby hold $\omega_a = \dot{\Theta}_a$ and $\omega = \dot{\Theta}$, where the superscript dot notation means differentiation with respect to time t. The distributed mass of the shaft S_h and the effect of gravity are neglected. A rectangular coordinate system O-xyz is stationary, and its z-axis coincides with the center line of two ball bearings. The point S is located at the origin O when the shaft has no deformations. In Fig. 4.1, G-XYZ is a movable rectangular coordinate system parallel to O-xyz, and its origin G is the center of gravity of the rotor D. The axes x_1, x_2, and x_3 fixed on the rotor D are the principal axes of inertia; the x_3-axis, the polar axis, is inclined by τ from the straight line GT parallel to tangent of the deflection curve at the point S. The azimuth direction of this dynamic unbalance τ is in advance by η to the sense of shaft rotation from the x_1-axis. The center of gravity G, furthermore, is in deviating by e from the point S, and its direction is in advance by ξ to the sense of shaft rotation from the x_1-axis. The moment of inertia about the x_1-axis as well as x_2-axis is I, and that about x_3-axis is I_p.

When the flexible shaft has some deformations, the point S deviates by x, y in the x-, y-directions, and the tangent at the point S of the deflection curve is θ. Let θ_x and θ_y be the projections of θ to the xz- and yz-planes, respectively. The torsional angle of shaft is defined as the difference between the rotational angle Θ_a at the point A and that Θ at the point S:

$$\theta_t = \Theta - \Theta_a \,. \tag{4.1}$$

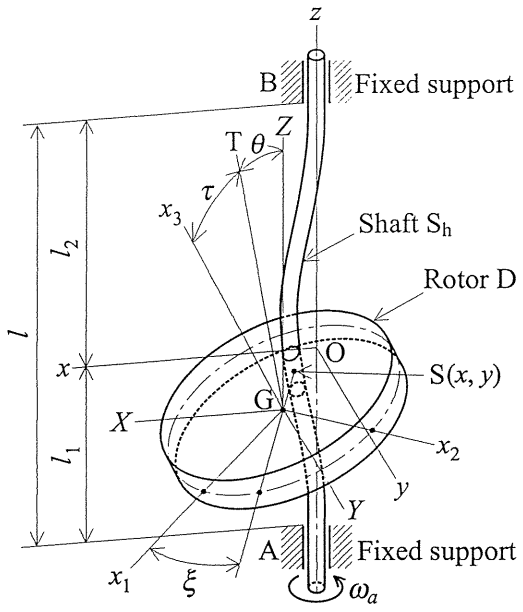

Fig. 4. 1. Rotor-shaft and coordinate systems (x_1-, x_2-, and x_3-axes are three principal axes of inertia of rotor, $\overline{GS} = e$ is eccentricity, and line GT is the tangent of shaft deformation curve at point S and is in G-x_1x_3 plane.).

We assume that the non-dimensional eccentricity e/l and the dynamic unbalance τ are small quantities of the same order as the deflection, the angle of deflection, and the angle of torsion. Thus, the equations of motion in this chapter are derived with an accuracy to the second-order of these small quantities. Now we introduce the following complex numbers:

$$z = (x + iy)/l,\ \theta_z = \theta_x + i\theta_y, \tag{4.2}$$

in which $i = \sqrt{-1}$.

Let α, γ, and δ be the spring constants for lateral displacements of the shaft, δ_t be the spring constant for torsion of the shaft, and c_1, c_2, and c_3 be the viscous damping coefficients for translation, inclination, and rotation of the rotor, respectively.

4.2.2 *Equations of motion*

Here we introduce the following non-dimensional parameters:

$$\begin{aligned}
&e' = e/l,\ T_r' = T_r/(\alpha l^2),\ \gamma' = \gamma/(\alpha l),\ \delta' = \delta/(\alpha l^2),\ \delta_t' = \delta_t/(\alpha l^2),\\
&c_1' = c_1/\sqrt{m\alpha},\ c_2' = c_2/(l^2\sqrt{m\alpha}),\ c_3' = c_3/(l^2\sqrt{m\alpha}),\\
&\omega_a' = \omega_a/\sqrt{\alpha/m},\ \omega' = \omega/\sqrt{\alpha/m},\ t' = t\sqrt{\alpha/m},\\
&I' = I/(ml^2),\ I_p' = I_p/(ml^2).
\end{aligned} \tag{4.3}$$

Hereafter, the primes expressing non-dimensional quantities in Eq. (4.3) are omitted.

The kinetic energy of the rotor is given as the sum of the energy for translation and that for rotational motion. The potential energy of the flexible shaft is derived by using theory of elasticity to bending and torsion[37]. The dissipation function is calculated under the assumption that the rotor is subjeted to viscous frictions for the translation, the rotational motion about the polar axis, and that about the axis perpendicular to the polar axis. Substituting the kinetic energy, the potential one, and the dissipation function into Lagrange's equations of motion, we obtain the following equations of motion:

$$\ddot{z} + z + \gamma\theta_z = -c_1\dot{z} - i\delta_t\theta_t\theta_z + e\left\{\dot{\Theta}^2 - i(\Theta + c_1\dot{\Theta})\right\}\exp\{i(\Theta + \xi)\}\,, \tag{4.4}$$

$$\begin{aligned} &I\ddot{\theta}_z - iI_p\dot{\Theta}\dot{\theta}_z + \delta\theta_z + \gamma z \\ &\quad = -c_2\dot{\theta}_z + i\delta_t\theta_t z + \frac{i\theta_z}{2}(I_p\Theta + c_3\dot{\Theta}) \\ &\quad + \tau\left[(I - I_p)\dot{\Theta}^2 - i\left\{(I - I_p)\Theta + (c_2 - c_3)\dot{\Theta}\right\}\right]\exp\{i(\Theta + \eta)\}\,, \end{aligned} \tag{4.5}$$

$$\begin{aligned} &I_p\Theta + c_3\dot{\Theta} \\ &\quad = T_r + \mathrm{Im}\left[\frac{1}{2}I_p\ddot{\theta}_z\bar{\theta}_z - \left\{e\ddot{z}\exp(-i\xi) + \tau(I - I_p)\ddot{\theta}_z\exp(-i\eta)\right\}\exp(-i\Theta)\right], \end{aligned} \tag{4.6}$$

where $\bar{\theta}_z$ is a conjugate complex number of θ_z, Im[ ] represents an imaginary part in [ ], and the superscript dot notation means differentiation with respect to non-dimensional time t. The torque T_r is given by the following equation:

$$T_r = -\delta_t\theta_t - \delta_t(y\theta_x - x\theta_y)\,. \tag{4.7}$$

The rotating shaft system has four natural angular frequencies for the whirling vibrations. Let these frequencies be p_1, p_2, p_3, and p_4 in order of size.

4.2.3 *Rotating angle*

In this analysis, the angular acceleration λ is constant. Therefore, the rotating speeds at the points A and S are calcurated as

$$\omega_a = \omega_{a0} + \lambda t, \quad \omega = \omega_a + \dot{\theta}_t\,, \tag{4.8}$$

where ω_{a0} is the initial rotating speed of the point A.

Furthermore, the rotating angle at the point A is determined by integrating Eq. (4.8):

$$\Theta_a = \omega_{a0}t + \frac{1}{2}\lambda t^2\,, \tag{4.9}$$

where $\Theta_a = 0$ at time $t = 0$.

4.2.4 *Angle of torsion*

The angle of torsion θ_t consists of the following two components: one is a part determined by the angular acceleration λ and the damping coefficient of torsion c_3, another is a part influenced by whirling vibration of shaft. Let the former part be θ_{t1} and the latter θ_{t2}. Then the angle θ_t can be written as

$$\theta_t = \theta_{t1} + \theta_{t2} . \tag{4.10}$$

The torsional angle θ_{t1} is a particular solution of Eq. (4.6) neglected the second-order of small quantities:

$$\theta_{t1} = -\frac{1}{\delta_t}\{I_p\lambda + c_3(\omega_{a0} + \lambda t - c_3\lambda/\delta_t)\} , \tag{4.11}$$

which changes smoothly with time. When θ_{t1} is given by Eq. (4.11), an equation for θ_{t2} becomes as follows:

$$\begin{aligned} I_p\ddot{\theta}_{t2} + \delta_t\theta_{t2} = & -c_3\dot{\theta}_{t2} + \delta_t(\theta_x y - \theta_y x) - \frac{1}{2}I_p(\ddot{\theta}_x\theta_y - \ddot{\theta}_y\theta_x) \\ & + \tau(I - I_p)\{\ddot{\theta}_x \sin\Theta - \ddot{\theta}_y \cos\Theta\} + e\{\ddot{x}\sin(\Theta + \xi) - \ddot{y}\cos(\Theta + \xi)\} . \end{aligned} \tag{4.12}$$

If the right hand side of Eq. (4.12) changes with natural frequency p_t, then the torsional vibration will resonate.

4.3 *Numerical results*

4.3.1 *Parameters*

Numerical integration for Eqs. (4.4), (4.5), and (4.12) explains the influences of the angular acceleration or the damping coefficient on the torsional vibration.

The common parameters' values when integrating are as follows:

$$\left.\begin{aligned} & I = 0.0534,\ I_p = 0.1034,\ l_1 = 0.200,\ \gamma = -0.0923,\ \delta = 0.0164, \\ & \delta_t = 0.00256,\ e = 1.0 \times 10^{-4},\ \tau = 4 \times 10^{-4},\ \eta = 0^\circ. \end{aligned}\right\} \tag{4.13}$$

Using of these parameters determines the critical speed for whirling,

$$\omega_{ac} = 0.925, \tag{4.14}$$

and the natural angular frequency for torsion,

$$p_t = 0.157 \tag{4.15}$$

4.3.2 *Torsional vibration in passing critical speed*

(i) Case of acceleration

Figure 4.2 shows the the amplitude of whirling $A = |z|$ and the torsional angle θ_{t2} to the rotating speed ω_a with the acceleration $\lambda = 0.20 \times 10^{-3}$ from 0.70 to 1.40. The initial condition for numerical integration is determined from the stationary solution when starting acceleration. The angle θ_{t2} starts to fluctuate at $\omega_a = \omega_{c1}$ where the amplitude A grows. The whirling amplitude A repeats alternately increase and decrease after its peak. The torsional vibration θ_{t2} becomes larger suddenly in $\omega_a = 1.10 \sim 1.15$ and decreases monotonously after.

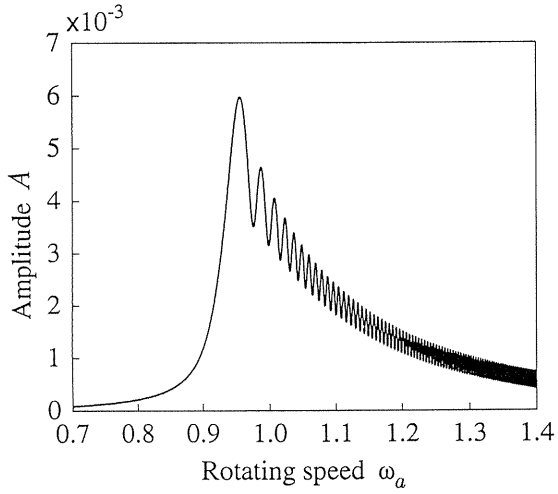

Fig. 4. 2. (a) Whirling amplitude

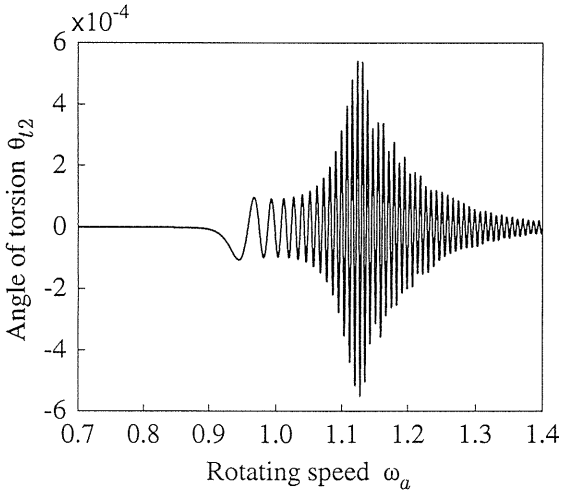

Fig. 4. 2. (b) Torsional vibration

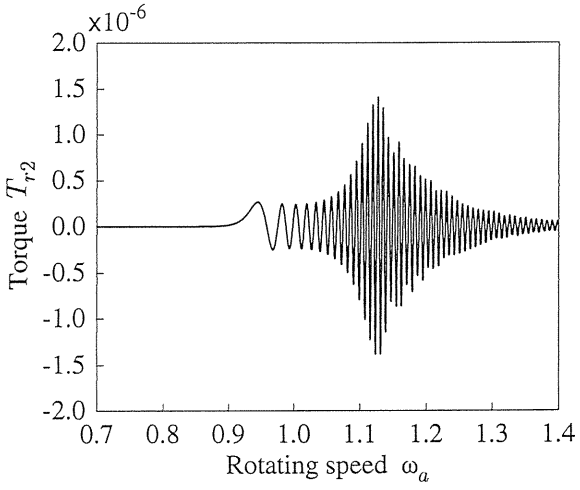

(c) Driving torque

Fig. 4. 2. Changes of whirling amplitude and torsional vibration in acceleration ($\lambda = 2 \times 10^{-4}$, $c_1 = c_2 = 1 \times 10^{-3}$, $c_3 = 5 \times 10^{-4}$).

We can notice by detail observation to Fig. 4.2 that θ_{t2} becomes negative or positive according as A increases or decreases. The driving torque T_{r2} also changes similarly to θ_{t2}, and its change is almost $-\delta_t\theta_{t2}$, then the term $-\delta_t(y\theta_x - x\theta_y)$ does not seem to effect on θ_{t2}.

(ii) Case of deceleration

Figures (4.3a) and (4.3b) show the patterns of the amplitude A and the angle θ_{t2} to the rotating speed ω_a with the constant deceleration $\lambda = -0.20 \times 10^{-3}$ from 1.20 to 0.50. The maximum amplitude of shaft whirling is slightly smaller than that in acceleration, while its periodical change is faster than that in acceleration. A torsional vibration of the rotating shaft starts after the critical speed ω_{ac}, and its peak appears around $\omega_a = 0.72$. The peak is about half of that in acceleration.

We have shown the typical patterns of change of the whirling amplitude and angle θ_{t2} in Figs. (4.2) and (4.3). The maximum value of θ_{t2} around $\omega_a = 1.13$ in acceleration and $\omega_a = 0.72$ in deceleration can be made smaller than the peak value just after passing $\omega_a = \omega_{ac}$ by some parameters of the system. But we take the former value for θ_{t2max}, "the maximum value of θ_{t2}."

4.3.3 *Effect of angular acceleration*

Figure 4.4 shows how the angle θ_{t2max} depends upon the angular acceleration λ. Both black triangles and white ones represent the first peak of the angle θ_{t2} appearing in passing the critical speed $\omega_a = \omega_{ac}$. These peaks are almost the same value both in acceleration and in deceleration for an absolute value of angular acceleration $|\lambda|$.

Both black circles and white ones represent the angle θ_{t2max} appearing after passing the critical speed. The angle θ_{t2max} is very small for the smaller $|\lambda|$ near zero. It grows rapidly and reaches its maximum for a little larger $|\lambda|$, and decreases for much larger $|\lambda|$. And among all range of $|\lambda|$ shown in Fig. 4.4, θ_{t2max} in acceleration is always larger than that in deceleration.

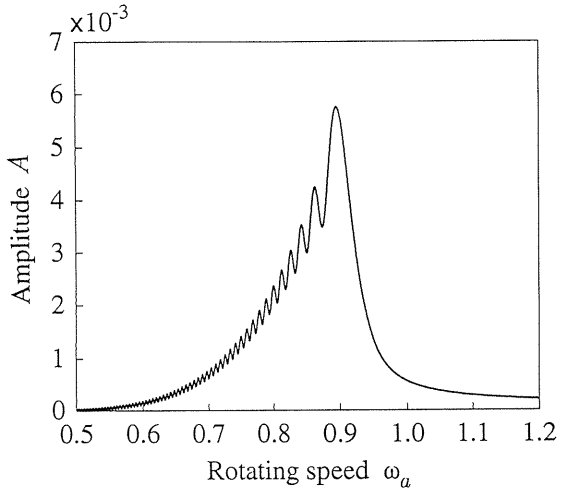

(a) Whirling amplitude

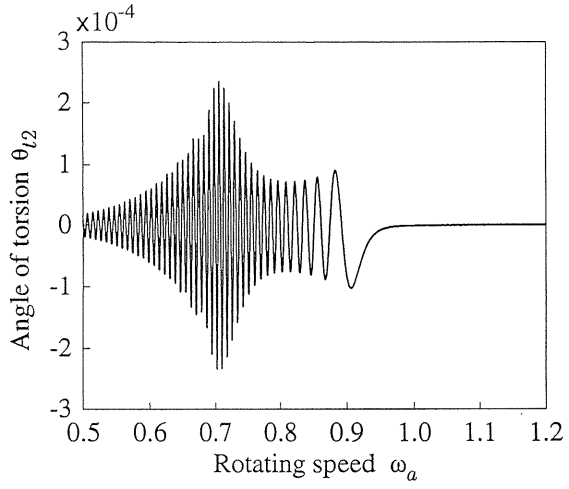

(b) Torsional vibration

Fig. 4. 3. Changes of whirling amplitude and torsional vibration in deceleration ($\lambda = -2 \times 10^{-4}$, $c_1 = c_2 = 1 \times 10^{-3}$, $c_3 = 5 \times 10^{-4}$).

According to Fig. 4.4, it is not better to pass the critical speed by using too small $|\lambda|$ because the peak of θ_{t2} and that of shaft whirling A at $\omega_a = \omega_{ac}$ becomes too large, though θ_{t2max} becomes very small. Also using larger $|\lambda|$ is no longer good because it makes θ_{t2max} larger. The parameters used in Fig. 4.4 let us know that the best values of the angular acceleration λ are $\lambda \approx 0.07 \times 10^{-3}$ in acceleration and $\lambda \approx -0.13 \times 10^{-3}$ in deceleration, which λs make the maximum value of these two peaks of θ_{t2} in $\omega_a = \omega_{ac}$ and θ_{t2max} the smallest.

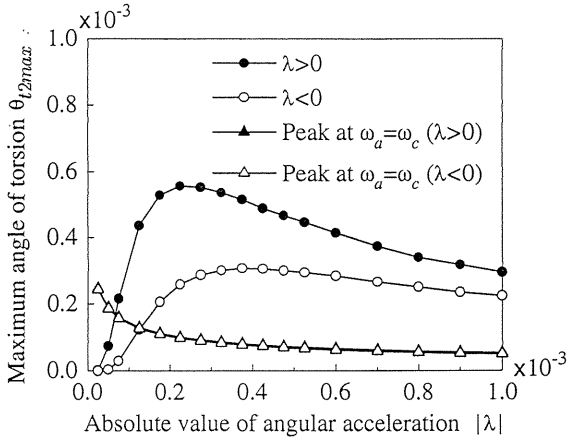

Fig. 4. 4. Effect of angular acceleration on maximum angle of torsion ($c_1 = c_2 = 1.0 \times 10^{-3}$, $c_3 = 0.5 \times 10^{-3}$).

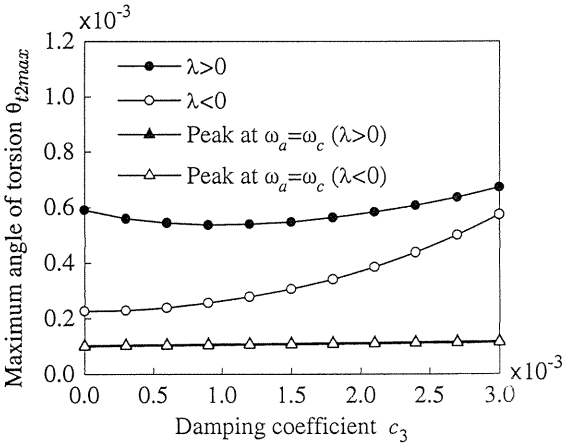

Fig. 4. 5. Effect of damping coefficient for shaft rotation ($|\lambda| = 0.2 \times 10^{-3}$, $c_1 = c_2 = 1.0 \times 10^{-3}$).

4.3.4 *Effect of damping coefficient for rotation*

Effect of the damping coefficient for rotation c_3 on the angle θ_{t2max} is shown in Fig. 4.5. The peak at $\omega_a \approx \omega_{ac}$ is hardly effected by c_3. As the value of c_3 increases, the value of θ_{t2max} becomes larger in deceleration, but it changes slightly in acceleration. The amplitude of torsional vibration does not always decrease as c_3 increases.

4.3.5 *Effect of damping coefficients for translation and inclination*

Effect of damping coefficients for translation c_1 and inclination c_2 is shown Fig. 4.6. The peaks of θ_{t2} at $\omega_a \approx \omega_{ac}$ are not effected by both c_1 and c_2, but they are clearly

effected by c_1 and c_2. For larger values of c_1 and c_2 (larger than 3.5×10^{-3} in acceleration and than 1.5×10^{-3} in deceleration), the value of θ_{t2max} is smaller than the peak value at $\omega_a = \omega_{ac}$.

4.4 *Mechanism for torsional vibration*

Figures 4.2(a) and 4.3(a) show that the amplitude of shaft A whirling after passing critical speed changes periodically like beats. This beating phenomenon occurs because the whirling vibration after passing through the critical speed consists of two vibrations: one is forced vibration by unbalance of rotor and the other is free vibration. The frequency of this

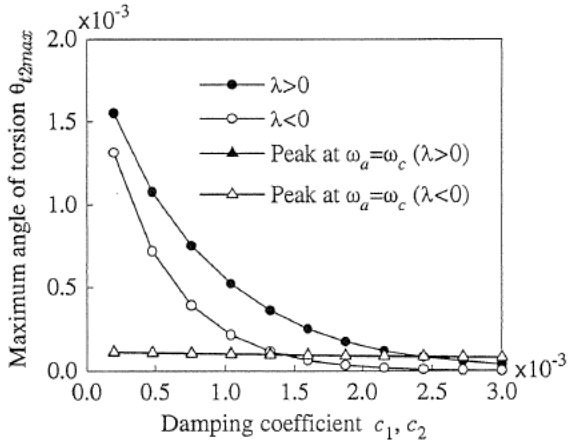

Fig. 4. 6. Effect of damping coefficient for translation and inclination ($|\lambda| = 0.2 \times 10^{-3}$, $c_3 = 0.5 \times 10^{-3}$).

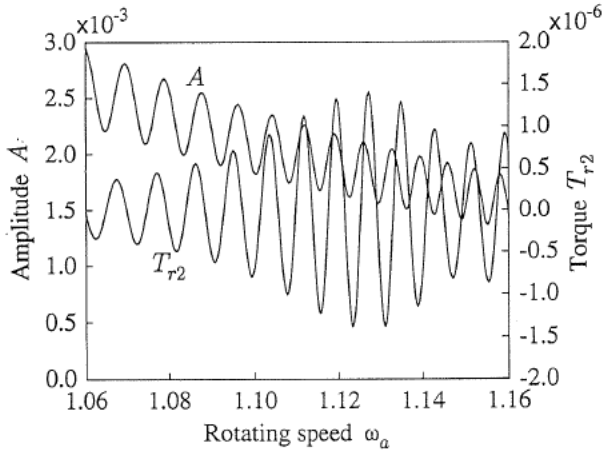

Fig. 4. 7. Change of whirling amplitude and driving torque (closed pattern of Fig. 4.2).

forced vibration is ω_a, the rotating speed. The frequency of free vibration just after passing critical speed ω_{ac} is mainly p_2, because at the rotating speed ω_{ac} there appears a resonance of forced vibration with frequency ω_a and one of natural angular frequencies p_2. The resonance gives the maximum whirling amplitude $A_{\max}$. Then vibrating mode of p_2 becomes dominating, and the shaft deformation at that time is the initial condition for free vibration of the shaft. Therefore, the changing frequency of shaft whirling just after passing critical speed is almost $\omega_a - p_2$ in acceleration and $p_2 - \omega_a$ in deceleration.

Now consider on the relation between whirling amplitude A and a flucuating component of driving torque T_{r2}. The rotating speed ω_a approaches the critical speed ω_{ac} and amplitude A is increasing, with the maximum gradient of A at the peak of torque T_{r2}. And T_{r2} does not turns into negative until A start to decrease. This relation of phase between amplitude A and torque T_{r2} shows the best efficiency of work done by driving torque at the shaft end A to change the energy of the rotor-shaft system. But this relation is not maintained after angle of torsion becomes large.

Figure 4.7 is the close pattern of Fig. 4.2 from $\omega_a = 1.06 \sim 1.16$. The changing frequency of amplitude A increases and when it coincides with natural frequency of torsional vibration p_t, the shaft starts to vibrate torsionally in its natural frequency p_2. Then there is no more that phase relation, and the efficiency of work by the driving torque becomes worse. Therefore large change of driving torque is needed, and the torque change makes this torsional vibration.

4.5 *Conclusions*

We have derived the equations of motion of a symmetrical rotor-shaft system to the second order of shaft deformations, and then integrated them numerically to analyse the small component of the torsional vibration of the shaft. The results are summerized as follows:

(1) By using the equations of motion to the second order of small quantities, the smaller component of torsional vibration can be derived.

(2) The moments of restoring force and those derived from the eccentricity make a small vibration component of torsion.

(3) The amplitude of torsional vibration becomes large at the rotating speed equal to the sum of the natural angular frequencies of whirling and torsion.

Chapter 5. Torsional Vibration of an Asymmetrical Rotor-Shaft after Passing through its Critical Speed of Whirling[58,59]

5.1 *Introduction*

When a rotating shaft passes its critical speed of whirling, it is well-known that the amplitude of whirling reaches the maximum and changes periodically, and that the frequency of the change becomes higher as the rotating speed of the shaft leaves the critical speed[7]. In this case, the torsional angle is opposite in sense according to increase or decrease in the whirling amplitude[46]. The torsional vibration makes a resonanse when the frequency of change of whirling amplitude coincides with a natural frequency of the torsional vibration of the shaft. If the rotor is asymmetrical, the frequency of change of whirling amplitude has also the component twice as that in a symmetrical rotor-shaft system[18]. Then the torsional vibration of the shaft may resonate at two different rotating speeds. It should be noted that this torsional vibration may occur only by passing the critical speed of whirling under a constant angular acceleration.

The present rotor-shaft system is a simple one that consists of a symmetrical and flexible shaft and an asymmetrical rotor mounted on the shaft. Both ends of the shaft are fixedly supported. First, equations of motion of the system will be derived. Then, they will be analysed by applying asymptotic method[45]. The numerical results show that the torsional vibration of a shaft mounting an asymmetrical rotor has different character from that of a symmetrical rotor-shaft system.

5.2 *Asymmetrical rotor-shaft system and rotating angles*

5.2.1 *Asymmetrical rotor-shaft system*

Figure 5.1 shows the asymmetrical rotor-shaft system and its co-ordinate system. The shaft S_h is an elastic rod of length l with a uniform circular cross section. It is fixedly supported at both ends, A and B. And the shaft is driven at the point A. An asymmetrical rotor D is mounted at point S of the shaft. The distance from the driving point A to S is l_1 and the distance from S to the another end B is l_2. Three principal axes of inertia moment of rotor D are x_1, x_2 and x_3, and three moments of inertia about these principal axes are I_1, I_2 and I_p, respectively. These axes x_1 and x_2 are determined so that I_1 might be larger than I_2. Co-ordinate system O-xyz is stationary, and its z-axis coincides with the center line of the shaft when the shaft has no deformation. Co-ordinate system G-XYZ is parallel to O-xyz. The origin G is the center of gravity of the rotor D. Angular position of the eccentricity of rotor $\overline{GS} = e$ moves according to the deflection or rotation of the shaft and is in advance by ξ to the sense of shaft rotation from the x_1-axis. The dynamic unbalance of the rotor τ is the angle between the x_3-axis and the line $\overline{GT}$ which is parallel to the tangent of the shaft deflection curve at point S. The azimuth direction of this dynamic unbalance is in advance by η to the sense of shaft rotation from the x_1-axis.

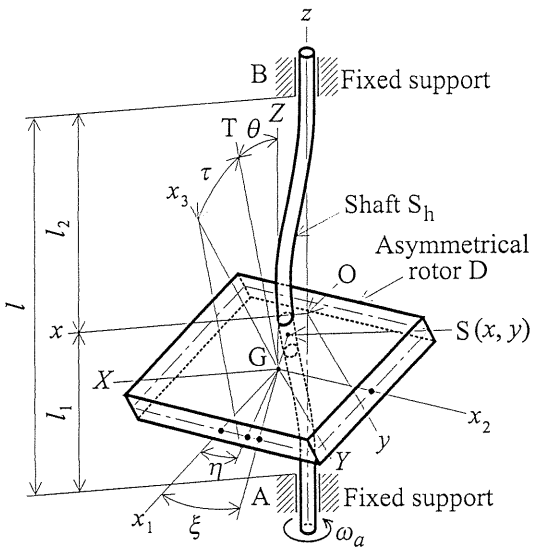

Fig. 5. 1. Asymmetrical rotor-shaft and coordinate systems (x_1, x_2, and x_3 are three principal axes of inertia. $\overline{GS} = e$ is eccentricity and τ is dynamic unbalance. Line GT is parallel to the tangent at the point S of the shaft deflection curve).

5.2.2 *Rotating angles*

The angle of rotation at point A is defined as Θ_a and that at point S is Θ. The angle of shaft torsion is defined as $\theta_t = \Theta - \Theta_a$. Assuming that the angular acceleration λ at the driving end A is constant, we have the following equations:

$$\dot{\omega}_a = \lambda\,, \quad \omega_a = \lambda t + \omega_{a0}\,, \quad \Theta_a = \frac{1}{2}\lambda t^2 + \omega_{a0} t\,, \tag{5.1}$$

$$\dot{\omega} = \lambda + \ddot{\theta}_t\,, \quad \omega = \lambda t + \omega_{a0} + \dot{\theta}_t\,, \quad \Theta = \frac{1}{2}\lambda t^2 + \omega_{a0} t + \theta_t\,, \tag{5.2}$$

in which ω_a is the rotating speed at A and ω is that at S, and ω_{a0} is the initial rotating speed at point A.

5.2.3 *Shaft deflection and angle of deflection*

Let the components of the shaft deflection along the x- and y-axis be x and y, and the projections of the angle of deflection to the xz- and yz- planes be θ_x and θ_y, respectively. By using the unit of imaginary number $i = \sqrt{-1}$, we introduce the following complex numbers representing the deflection and the angle of deflection of shaft:

$$z = x + iy\,, \quad \theta_z = \theta_x + i\theta_y\,. \tag{5.3}$$

5.3 *Equations of motion and parameters*

Let α, γ and δ be the spring constants for lateral displacement of the shaft. The rotor is subjected to viscous frictions against translation, inclination, and rotation. Let these damping coefficients be c_1, c_2, and c_3, respectively. Now we introduce the following non-dimensional parameters:

$$\begin{aligned}
&I' = (I_1 + I_2)/(2ml^2),\ I_p' = I_p/(ml^2),\ \Delta I' = (I_1 - I_2)/(2ml^2),\\
&e' = e/l,\ \gamma' = \gamma/(\alpha l),\ \delta' = \delta/(\alpha l^2),\ \delta_t' = \delta_t/(\alpha l^2),\\
&c_1' = c_1/\sqrt{m\alpha},\ c_2' = c_2/(l^2\sqrt{m\alpha}),\ c_3' = c_3/(l^2\sqrt{m\alpha}),\\
&\lambda' = \lambda/(\alpha/m),\ p' = p/\sqrt{\alpha/m},\ \omega_a' = \omega_a/\sqrt{\alpha/m},\ \omega' = \omega/\sqrt{\alpha/m},\\
&z' = z/l,\ t' = t\sqrt{\alpha/m}.
\end{aligned} \tag{5.4}$$

Hereafter, the primes which express non-dimensional parameters in Eq. (5.4) are omitted.

Angle of torsion θ_t is divided into two parts θ_{t1} and θ_{t2} as

$$\theta_t = \theta_{t1} + \theta_{t2}\,, \tag{5.5}$$

where θ_{t1} is the part which changes monotonously with time, given by

$$\theta_{t1} = -\frac{1}{\delta_t}\{I_p\lambda + c_3(\omega_{a0} + \lambda t - c_3\lambda/\delta_t)\}\,. \tag{5.6}$$

The quantity θ_{t2} is the part whose vibration may resonate at some rotating speeds, and it is determined by differential equations shown later.

The kinetic energy of the rotor is given as the sum of the kinetic energy for translation and that for rotational motion. The potential energy of the flexible shaft is given by applying the theory of elasticity to bending and torsion[37]. The dissipation function is calculated under an assumption that the rotor is subjected to viscous frictions for the translation, the rotational motion about the polar axis and that about the axis perpendicular to the polar axis. Neglecting a distributing mass of the shaft and the gravity, substitute the kinetic energy, the potential one and dissipation function into Lagrange's equations of motion. Then we obtain the following equations of motion:

$$\ddot{z} + z + \gamma\theta_z = -c_1\dot{z} - i\delta_t\theta_t\theta_z + e\{\omega^2 - i(\dot{\omega} + c_1\omega)\}\exp\{i(\Theta + \xi)\}\,, \tag{5.7}$$

$$\begin{aligned} I\ddot{\theta}_z - iI_p\omega\dot{\theta}_z + \delta\theta_z + \gamma z &= -c_2\dot{\theta}_z + i\delta_t\theta_t\left(z - \frac{1}{2}\theta_z\right) \\ &+ \tau\left[(I - I_p)\omega^2 - i\{(I - I_p)\dot{\omega} + (c_2 - c_3)\omega\}\right]\exp\{i(\Theta + \eta)\} \\ &+ \Delta I\left(\ddot{\bar{\theta}}_z + 2i\omega\dot{\bar{\theta}}_z\right)\exp(i2\Theta) + \tau\Delta I(\omega^2 - i\dot{\omega})\exp\{i(\Theta - \eta)\}\,, \end{aligned} \tag{5.8}$$

$$\begin{aligned} &I_p\ddot{\theta}_{t2} + c_3\dot{\theta}_{t2} + \delta_t\theta_{t2} \\ &= \mathrm{Im}\left[\frac{1}{2}I_p\ddot{\theta}_z\bar{\theta}_z - \Delta I\dot{\theta}_z^{\,2}\exp\{-i2\Theta\} - \delta_t z\bar{\theta}_z - e\ddot{z}\exp\{-i(\Theta + \xi)\}\right. \\ &\left. -\tau(I - I_p)\ddot{\theta}_z\exp\{-i(\Theta + \eta)\} - \tau\Delta I\ddot{\theta}_z\exp\{-i(\Theta - \eta)\}\right]\,, \end{aligned} \tag{5.9}$$

where $\bar{\theta}_z$ is a complex conjugate of θ_z, Im[ ] represents an imaginary part in [ ], and the superscript dot means differentiation with respect to non-dimensional time t. Equations (5.7), (5.8) and (5.9) have an accuracy of the second-order of the small parameters and variables. This accuracy is needed in order to analyse the torsional vibration. The driving torque T_r is given by the following equation:

$$T_r = -\delta_t\{\theta_t + \mathrm{Im}[z\bar{\theta}_z]\}\,. \tag{5.10}$$

5.4 *Asymptotic solution*

5.4.1 *Whirling vibration*

The rotating shaft has four natural angular frequencies for whirling vibration. Let these frequencies be p_1, p_2, p_3 and p_4 in order of size. We deal with the case that the shaft system is passing through its critical speed $\omega = p_2$ under the constant angular acceleration. The asymptotic method is applied to analyse the non-linear Eqs. (5.7), (5.8) and (5.9). The rotating shaft is assumed to vibrate with single whirling mode of frequency p_2. Under this assumption, we can construct the asymptotic solutions for equations of motion. The first approximate equations are expressed as the following equations[45]:

$$z = A_k\exp\{i(\Theta + \Phi_k)\}\,, \quad \theta_z = \kappa_k A_k\exp\{i(\Theta + \Phi_k)\}\,, \tag{5.11}$$

$$\left.\begin{aligned} \dot{A}_k &= -\zeta_k A_k + e\mu_k \sin(\Phi_k - \xi) + \tau\nu_k \sin(\Phi_k - \eta) + \Delta I\sigma_k A_k \sin 2\Phi_k , \\ \dot{\Phi}_k &= p_k - \omega + \frac{e\mu_k}{A_k}\cos(\Phi_k - \xi) + \frac{\tau\nu_k}{A_k}\cos(\Phi_k - \eta) + \Delta I\sigma_k \cos 2\Phi_k , \end{aligned}\right\} \tag{5.12}$$

where

$$\kappa_k = -(1 - p_k^2)/\gamma , \tag{5.13}$$

$$\zeta_k = \frac{2(c_1 + c_2\kappa_k^2)p_k + \delta_t\theta_t\kappa_k^2 + \lambda\beta_k}{4p_k + 2\kappa_k^2(2Ip_k - I_p\omega)} , \tag{5.14}$$

$$\mu_k = -\frac{\omega^2}{p_k + \omega + \kappa_k^2\{I(p_k + \omega) - I_p\omega\}} , \tag{5.15}$$

$$\nu_k = -\frac{(I - I_p)\kappa_k\omega^2}{p_k + \omega + \kappa_k^2\{I(p_k + \omega) - I_p\omega\}} , \tag{5.16}$$

$$\sigma_k = -\frac{\kappa_k^2 p_k(2\omega - p_k)}{\omega\{2 + (2I - I_p)\kappa_k^2\}} , \tag{5.17}$$

$$\beta_k = -\frac{2(\delta_t\theta_t + c_3\omega)}{I_p}\frac{\mathrm{d}p_k}{\mathrm{d}\omega}\left\{1 + I\kappa_k^2 + \frac{2\kappa_k p_k}{\gamma}(2Ip_k - I_p\omega)\right\} . \tag{5.18}$$

The term $\mathrm{d}p_k/\mathrm{d}\omega$ can be derived as

$$\frac{\mathrm{d}p_k}{\mathrm{d}\omega} = \frac{I_p p_k^2(1 - p_k^2)^2}{(1 - p_k^2)^2(\delta + Ip_k^2) + \gamma^2(3p_k^2 - 1)} \tag{5.19}$$

from the following equation of natural frequency:

$$(1 - p^2)(\delta + I_p\omega p - Ip^2) - \gamma^2 = 0 . \tag{5.20}$$

By conversion of variables

$$u_k = A_k\cos\Phi_k , \quad v_k = A_k\sin\Phi_k , \tag{5.21}$$

Eq. (5.12) can be rewritten as following:

$$\left.\begin{aligned} \dot{u}_k &= -\zeta_k u_k + \{\Delta I\sigma_k - (p_k - \omega)\}v_k - e\mu_k\sin\xi - \tau\nu_k\sin\eta , \\ \dot{v}_k &= \{\Delta I\sigma_k + (p_k - \omega)\}u_k - \zeta_k v_k + e\mu_k\cos\xi + \tau\nu_k\cos\eta . \end{aligned}\right\} \tag{5.22}$$

5.4.2 *Torsional vibration*

The deflection and inclination of the shaft are given by Eqs. (5.11) and (5.12), or by (5.22). Substitute them into the Eq. (5.9) and ignore small quantities above the second-order of e, τ, ΔI, ζ_k, c_3 and θ_t. Then, we obtain the following equation for torsional vibration θ_{t2}:

$$\begin{aligned} I_p\ddot{\theta}_{t2} + c_3\dot{\theta}_{t2} + \delta_t\theta_{t2} = \frac{1}{2}I_p\kappa_k(u_k^2 + v_k^2)\left(\dot{\omega}\frac{5p_k^2 - 1}{\gamma}\frac{dp_k}{d\omega} - 2\zeta_k\kappa_k p_k\right) \\ -(e\rho_k\sin\xi + \tau\vartheta_k\sin\eta)u_k + (e\rho_k\cos\xi + \tau\vartheta_k\cos\eta)v_k \\ + 2\Delta I(I_p\omega\sigma_k + p_k^2)\kappa_k^2 u_k v_k, \end{aligned} \tag{5.23}$$

where

$$\rho_k = \frac{1}{2}I_p\kappa_k^2\mu_k(p_k + \omega) + p_k^2,\ \vartheta_k = \kappa_k\left\{\frac{1}{2}I_p\kappa_k\nu_k(p_k + \omega) + (I - I_p)p_k^2\right\}, \tag{5.24}$$

and

$$\dot{\omega} = -\frac{1}{I_p}(\delta_t\theta_t + c_3\omega) \tag{5.25}$$

which has an accuracy of the first-order of small quantities.

5.5 *Numerical results*

5.5.1 *Parameters, critical speed and initial condition*

Here we integrate Eqs. (5.22) and (5.23) numerically, and analyse the effects of asymmetry of rotor $\Delta I/I$ and angular acceleration λ upon the torsional vibration θ_{t2}. Some values of the non-dimensional parameters are as the following:

$$\left.\begin{aligned} &I = 0.0534,\quad I_p = 0.1034,\quad \gamma = -0.0923,\quad \delta = 0.0164, \\ &\delta_t = 0.00256,\quad e = 6.0 \times 10^{-5},\quad \tau = 6.0 \times 10^{-5}, \\ &c_1 = c_2 = 4.0 \times 10^{-4},\quad c_3 = 1.0 \times 10^{-4}, \end{aligned}\right\} \tag{5.26}$$

the values of which are fixed throughout this chapter and other parameters are shown each time.

Since I_p is greater than I in Eq. (5.26), there is only one critical speed for whirling at $\omega_a = p_2$. This critical speed for whirling is calculated $\omega_{ac} = 0.9253$, and natural frequency for torsional vibration is $p_t = 0.1573$.

Initial condition for integration is a steady state at starting speed derived by putting $\dot{u}_k = \dot{v}_k = 0$ in the Eq. (5.22) for whirling, for torsional vibration putting $\theta_{t2} = \dot{\theta}_{t2} = 0$.

5.5.2 *Torsional vibration and change of whirling amplitude*

Figure 5.2 shows a typical pattern of torsional vibration θ_{t2} of a rotating shaft. For reference, the pattern of whirling amplitude A_2 is also shown. Dotted line shows a steady value

of A_2. In Fig. 5.2, angular acceleration at driving point A is $\lambda = 1.0 \times 10^{-4}$, and asymmetry of rotor is $\Delta I/I = 0.05$. This asymmetry is not so large, but it shows a different pattern from that shown in the Fig. 5.3 whose parameters except asymmetry $\Delta I/I$ are the same as those of the Fig. 5.2. We can find that θ_{t2} and A_2 change synchronously after passing through ω_{ac} to $\omega_a \approx 1.0$ in Fig. 5.2, ω_{ac} to $\omega_a \approx 1.1$ in Fig. 5.3. In Fig. 5.2, the first resonance peak of torsional vibration appears about $\omega_a = 1.03$. We named this peak ①. But in Fig. 5.3, ① does not appear. This shows that ① does not generate until the rotor has asymmetry. In both Figs. 5.2 and 5.3, another resonance peak ② appears nearly at $\omega_a = 1.12$. Whether ① or ② is

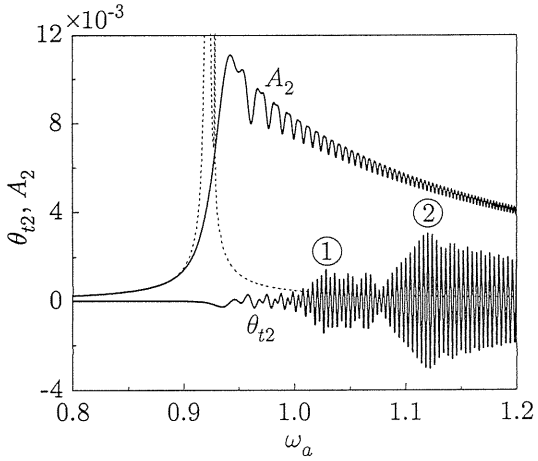

Fig. 5. 2. Torsional vibration in passing through the critical speed of whirling ($\Delta I/I = 0.05$, $\lambda = 1.0 \times 10^{-4}$, $\xi = 0$, $\eta = \pi$).

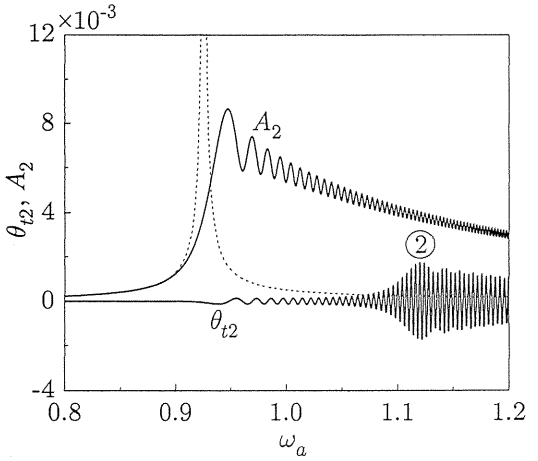

Fig. 5. 3. Torsional vibration in passing through the critical speed of whirling ($\Delta I/I = 0$, $\lambda = 1.0 \times 10^{-4}$, $\xi = 0$, $\eta = \pi$).

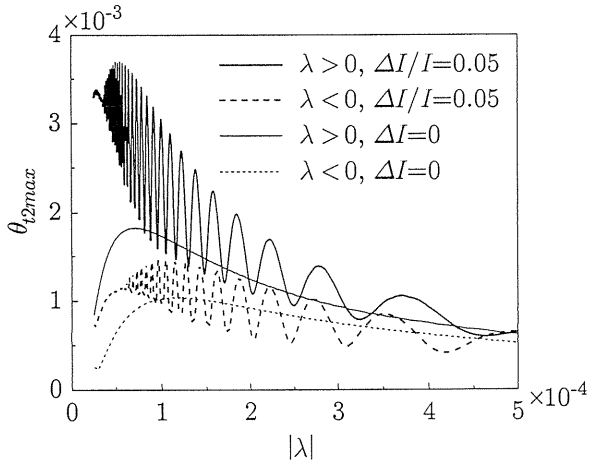

Fig. 5. 4. Effect of angular acceleration on the maximum amplitude of torsional vibration ($\xi = 0$, $\eta = \pi$).

larger depends on the values of angular acceleration λ, asymmetry of rotor $\Delta I/I$, angular position of eccentricity ξ, and so on.

5.5.3 *Critical speeds for torsional vibration*

When a symmetrical rotor-shaft system passes through its critical speed ω_{ac} for whirling, the whirling amplitude A_2 has one frequency component $\omega_a - p_2$ in acceleration or $p_2 - \omega_a$ in deceleration. In addition to this, A_2 in asymmetrical rotor-shaft system includes one more frequency component $2(\omega_a - p_2)$ in acceleration or $2(p_2 - \omega_a)$ in deceleration as shown in Fig. 5.2 because of asymmetry of rotor. If one of these two frequencies coincides with the natural frequency of torsional vibration p_t, the resonance of torsional vibration occurs. Then critical speeds for torsional vibration ω_{ct} are calculated in acceleration as the solution of the following equations,

$$2(\omega_{ct} - p_2) = p_t, \tag{5.27}$$

$$\omega_{ct} - p_2 = p_t, \tag{5.28}$$

and also in deceleration,

$$2(p_2 - \omega_{ct}) = p_t, \tag{5.29}$$

$$p_2 - \omega_{ct} = p_t. \tag{5.30}$$

The critical speeds from Eqs. (5.27) and (5.29) make resonance named ① and those from Eqs. (5.28) and (5.30) make ②. For the parameters shown in Eq. (5.26), each value of ω_{ct} from equations (5.27) ~ (5.30) is calculated as 1.0039, 1.0826, 0.8467, 0.7680, respectively. Figures 5.2 and 5.3 support these calculated results.

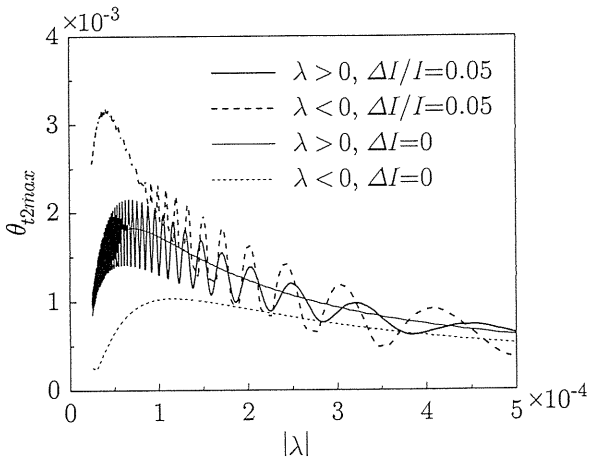

Fig. 5. 5. Effect of angular acceleration on the maximum amplitude of torsional vibration ($\xi = 0.5\pi$, $\eta = 1.5\pi$).

5.5.4 *Effects of angular acceleration*

The maximum amplitude of torsional vibration θ_{t2max} is effected by the angular acceleration λ. Figure 5.4 shows the result in case $\xi = 0$. The maximum amplitude θ_{t2max} in acceleration is larger than that in deceleration. In contrast with this, Figure 5.5 ($\xi = \pi/2$) shows that θ_{t2max} in acceleration is not always larger than that in deceleration especially in smaller $|\lambda|$. This means that angular position of eccentricity and angular acceleration effect on θ_{t2}.

Both Figs. 5.4 and 5.5 show that in asymmetrical rotor-shaft system θ_{t2max} fluctuates and approaches closer to that in symmetrical rotor-shaft system according to larger $|\lambda|$, and that in such case as smaller $|\lambda|$ about 1×10^{-4} a little change of $|\lambda|$ causes large change of θ_{t2}. It is because of the phase difference of torsional vibrations ① and ② causing θ_{t2max} larger or smaller. If ① and ② are in the same phase, θ_{t2max} becomes large, and if they are in the opposite phase, θ_{t2max} becomes small.

5.5.5 *Effects of angular position of eccentricity*

In asymmetrical rotor-shaft system, whirling amplitude changes according to the angular position of the eccentricity. So the amplitude of torsional vibration may also change according to the angular position of the eccentricity. Figure 5.6 shows effects of angular position of eccentricity ξ upon the maximum amplitude of torsional vibration θ_{t2max} with fixed relation $\eta = \xi + \pi$. The same result as shown in Fig. 5.6 is obtained in the case $\xi = \pi \sim 2\pi$ because of geometrical character of this system.

According to Fig. 5.6, both in acceleration and in deceleration θ_{t2max} increases and decreases once when ξ/π changes 0 to 1. In such region as $\xi/\pi \approx 0.4 \sim 0.8$, θ_{t2max} in asymmetrical rotor-shaft system is smaller than that in symmetrical rotor-shaft system when the rotating shaft is accelerated. The resultant vibration of torsion consists of the vibration caused by the eccentricity and the dynamic unbalance and that caused by the asymmetry. The two is in or out of phase by the magnitude of ξ.

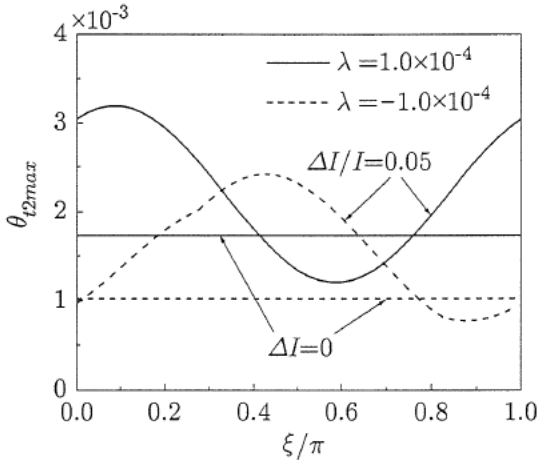

Fig. 5. 6. Effect of angular position of unbalance on the maximum amplitude of torsional vibration ($\eta = \xi + \pi$).

5.6 *Conclusions*

In this study we deal with the torsional vibration of an asymmetrical rotor-shaft system. The torsional vibration may occur twice after passing through the critical speed for whirling. First is caused by asymmetry of rotor and second is by eccentricity and dynamic unbalance of rotor.

In case of acceleration, the critical speeds for torsional vibration ω_{ct} are calculated as $\omega_{ct} = \omega_{ac} + p_t/2$ and $\omega_{ct} = \omega_{ac} + p_t$ where ω_{ac} is the critical speed for whirling and p_t is the natural frequency for torsion. In case of deceleration, the critical speeds are $\omega_{ct} = \omega_{ac} - p_t/2$ and $\omega_{ct} = \omega_{ac} - p_t$.

The amplitude of torsional vibration depends on the angular acceleration, the angular positions of eccentricity and dynamic unbalance, and the asymmetry of rotor.

Acknowledgement

The authors express thanks to Mr. S. Shirakura and Mr. H. Tozawa, bachelor course students in the academic year 1991, to Mr. K. Nakazato in 1992, and to Mr. K. Kawano in 1994, for their assistance in some of calculation and consideration.

The caluculation in chapter 3 was performed in Nagoya University Computation Center by using a subroutine RKF4AD of scientific libraries NUMPAC in 1992.

References

1) Rankine, W. J. McQ., *On the Centrifugal Whirling of Shafts*, The Engineer, Vol.**27** (1869-4), p.249.
2) Grammel, R., *Kritische Drehzahl und Kreiselwirkung*, Z. Ver. deutsch. Ing., Bd. **64**, Nr.44 (1920-10), S.911—914.
3) Stodola, A., *Steam and Gas Turbines*, McGraw-Hill Book (1927), pp.424—430.
4) Den Hartog, J. P., *Mechanical Vibrations (Fourth Edition)*, McGraw-Hill Book (1956), pp.225—229.
5) Kimball, A. L. and Hull, E. H., *Vibration Phenomena of a Loaded Unbalanced Shaft While Passing Through Its Critical Speed*, Trans. ASME, Vol.**47** (1925), pp.673—698.
6) Shimoyama, Y. and Yamamoto, T., *Researches of a shaft in passage through critical speed*, Trans. JSME, (in Japanese), **15**-50, I (1949-10), pp.113—121.
7) Dimentberg, F. M., *Flexural Vibration of Rotating Shafts*, Butterworths (1961), pp.42—60.
8) Yanabe, S. and Tamura, A., *Vibration of rotating shaft in passing through critical speed*, Trans. JSME, (in Japanese), **37**-294, 1 (1971-2), pp.268—275.
9) Yanabe, S., *Transitional vibration in passing through critical speed*, Kikaino-Kenkyū, (in Japanese), **29**-10 (1977-10), pp.1191—1196.
10) pp.1122—1130 of reference (4).
11) pp.155—186 of reference (7).
12) Taylor, H. D., *Critical-Speed Behavior of Unsymmetrical Shafts*, J. Appl. Mech., Trans. ASME, **7**-2 (1940-6), pp.A-71—A-79.
13) Brosens, P. J. and Crandall, S. H., *Whirling of Unsymmetrical Rotors*, J. Appl. Mech., Trans. ASME, **28**-3 (1961-9), pp.355—362.
14) Crandall, S. H. and Brosens, P. J., *On the Stability of Rotation of a Rotor with Rotationally Unsymmetric Inertia and Stiffness Properties*, J. Appl. Mech., Trans. ASME, **28**-4 (1961-12), pp.567—570.
15) Yamamoto, T. and Ota, H., *On the Vibrations of the Shaft Carrying an Asymmetrical Rotating Boby*, Bull. JSME, **6**-21, 1 (1963-2), pp.29—36.
16) Yamamoto, T. and Ota, H., *On the Forced Vibrations of the Shaft Carrying an Unsymmetrical Rotating Body (Response Curves of the Shaft at the Major Critical Speeds)*, Bull. JSME, **6**-23, 1 (1963-8), pp.412—420.
17) Yamamoto, T. and Ota, H., *On the Unstable Vibrations of a Shaft Carrying an Unsymmetrical Rotor*, J. App. Mech., Trans. ASME, **31**-3, 1 (1964-9), pp.515—522.
18) Kato, M. and Ota, H., *Whirling Vibration Passing through the Critical Speed of a Shaft with an Asymmetrical Rotor*, Trans. JSME, (in Japanese), **57**-543, C (1991-11), pp.3417—3422.
19) Ota, H., Kōno, K. and Mitsuya, Y., *On the Elimination of the Unstable Region of the Major Critical Speed in a Rotating Shaft Carrying an Unsymmetrical Rotor (Dynamic Effect of a Flexible Pedestal or Added Mass on the Shaft)*, Bull. JSME, **12**-51, (1969-6), pp.470—481.
20) Yamamoto, T., *On Sub-Harmonic and "Summed and Differential Harmonic" Oscillations of Rotating Shaft*, Trans. JSME, (in Japanese), **26**-164, 1 (1960-4), pp.612—620.
21) Yamamoto, T., Ishida, Y. and Ikeda, T., *Summed and Differential Harmonic Oscillations of Asymmetrical Shaft*, Trans. JSME, (in Japanese), **46**-405, C (1980-5), pp.465—472.
22) Yamamoto, T., *On the Critical Speeds of a Shaft*, Memoirs of Faculty of Engineering, Nagoya University, **6**-2 (1954-11), pp.106—174.
23) Tondl, A. *Dynamics of Rotating Shaft*, (Japanese Translation), Corona Publishing Co., (1971-5), pp.281—299.
24) Ota, H. and Mizutani, K., *Influence of Unequal Pedestal Stiffness on the Instability Regions of a Rotating Asymmetric Shaft*, J. App. Mech., Trans. ASME, **45**-2, 1 (1978-6), pp.400—408.
25) Ota, H., Mizutani, K. and Miwa, M., *Influence of Unequal Pedestal Stiffness on the Instability Regions of a Rotating Asymmetric Shaft (2nd Report, Inclination Vibrations with Effects of Gyroscopic Action)*, Bull. JSME, **23**-183, C (1980-9), pp.1514—1521.

26) Ishida, Y., Ikeda, T., Yamamoto, T. and Masuda, N., *Vibration of a Rotating Shaft Containing a Transverse Crack (1st Report, Variations of a Resonance Curve Due to Angular Position of an Unbalance at the Major Critical Speed)*, Trans. JSME, (in Japanese), **53**-488, C (1987-4), pp.925–932.
27) Stodola, A., *Kritische Drehzahlen rasch umlaufender Wellen*, Z. Ver. deutsch. Ing., Bd. **63**, Nr.36 (1919-9), S. 867–869.
28) Yamamoto, T. and Kōno, K., *On the Vibrations of Rotor with Variable Rotating Speed*, Bull. JSME, **13**-60, (1970-6), pp.757–765.
29) Fujii, S., *Whirling of an automobile propeller shaft at lower speeds (1st report)*, Trans. JSME, (in Japanese), **22**-115, 1 (1956-3), pp.178–181.
30) Porter, B., *A Theoretical Analysis of the Torsional Oscillation of a System Incorporating a Hooke's Joint*, J. Mech. Eng. Sci., **3**-4 (1961), pp.324–329.
31) Fujii, S., Shibata, H. and Shigeta, T., *Whirling of an Automobile Propeller Shaft at Lower Speeds (2nd Report)*, Trans. JSME, (in Japanese), **22**-119, 1 (1956-7), pp.489–491.
32) Ota, H. and Kato, M., *Lateral Vibrations of Rotating Shaft Driven by a Universal Joint (1st Report, Generation of Even Multiple Vibrations by Secondary Moment)*, Bull. JSME, **27**-231, (1984-9), pp.2002–2007.
Ota, H. and Kato, M., *Even Multiple Vibrations of a Rotating Shaft due to Secondary Moment of a Universal Joint*, Proc. 3rd. Int. Conf. Vibrations in Rotating Machinery, York, UK, (1984-9), pp.199–204.
33) Ota, H., Kato, M. and Mizuno, M., *Lateral Vibrations of an Asymmetrical Shaft Driven by Universal Joint (1st Report, Generation of Unstable Vibration and Expansion of Unstable Region by Angular Velocity Fluctuation)*, Bull. JSME, **29**-249, (1986-3), pp.916–923.
34) Nonami, K., Higashi, M. and Totani, T., *A Consideration of a Method of Passing through Critical Speed of Rotating Shaft Systems*, Trans. JSME, (in Japanese), **53**-496, C (1987-12), pp.2495–2500.
35) Nonami, K. and Miyashita, M., *Passing Problem of Critical Speed of Rotor with Consideration of Gyro Effect (3rd Report, In Case Shaft with Elastic Pedestals)*, Trans. JSME, (in Japanese), **46**-404, C (1980-4), pp.365–374.
36) Yamakawa, H., Nishioka, Y. and Suzuki, Y., *A Study on the Optimum Curve for Rotating Shaft Systems under Consideration of the Effect of Limited Power Supply*, Trans. JSME, (in Japanese), **52**-484, C (1986-12), pp.3108–3114.
37) Love, A. E. H., *A Treatise on the Mathematical Theory of Elasticity*, Dover Publications, (1927), pp.381–398.
38) Kato, M., Ota, H. and Nakamura, S., *Equations of motion of a shaft-rotor system with variable rotating speed*, Proc. of IMechE, 5th Int. Conf. on Vibrations in Rotating Machinery, Bath, UK, (1992-9), pp.469–473.
39) Yanabe, S., *Vibration of Rotating Shaft in Passing through Critical Speed (4th Report, Effect of Gyromoment)*, Trans. JSME, (in Japanese), **45**-398, C (1979-10), 1082–1091.
40) Yamakawa, H. and Murakami, S., *A Study on the Optimum Curve for Rotating Shaft Systems under Consideration of the Effect of Limited Power Supply (2nd Report)*, Trans. JSME, (in Japanese), **56**-527, C (1990-7), 1739–1744.
41) Macduff, J. N. and Curreri, J. R., *Vibration Control*, (Japanese Translation), Corona Publishing Co., (1967-8), pp.296–300.
42) pp.247–249 of reference (4).
43) Iwatsubo, T., Kamiyoshi, H. and Kawai, R., *Research on Critical Speed Passege Problem of Asymmetrical Shaft in Limited Power Supply (2nd Report, Effect of Phase Angle of Eccentricity of Shaft)*, Trans. JSME, (in Japanese), **40**-335, 1 (1974-7), 1908–1916.
44) Ota, H., Ishida, Y., Kato, Y. and Kondo, H., *Experiments on the Transient Vibration of an Unsymmetrical Shaft During Acceleration Through a Critical Speed*, Trans. JSME, (in Japanese), **53**-490, C (1987-6), pp.1160–1165.
45) Bogoliubov, N. N. and Mitropolisky, Y. A., *Nonlinear Vibration —Asymptotic Method—*, (Japanese Translation), Kyōritsu Publishing, (1965-8), pp.312–329.

46) Kato, M., Ota, H. and Nakamura, S., *Torsional Vibration of a Rotating Shaft driven by Constant Acceleration*, Proc. of the 5th Asia-Pacific Vibration Conference, Kitakyushu, Japan, (1993-11), pp.434—439.
47) Kato, M., Ota, H. and Nakamura, S., *Torsional Vibration of a Rotating Shaft in Passing through the Critical Speed of Whirling Vibration*, Trans. JSME, (in Japanese), **61**-584, C (1995-4), pp.1265—1270.
48) Iida, H., Tamura, A., Kikuchi, K. and Agata, H., *Bending-Torsional Coupled Vibration of Gear Shaft*, Trans. JSME, (in Japanese), **46**-404, C (1980-4), pp.375—382.
49) Iwatsubo, T., Arii, S. and Kawai, R., *Bending-Torsional Coupled Vibration of Shaft Coupled by Gears*, Trans. JSME, (in Japanese), **49**-422, C (1983-6), pp.929—936.
50) Kato, M., Ota, H. and Kato, R., *Lateral-Torsional Coupled Vibrations of a Rotating Shaft Driven by a Universal Joint (1st Report, Derivation of Equations of Motion and Asymptotic Analyses)*, JSME Int. J., **31**-1, C (1988-3), pp.68—74.
51) pp.170—206 of reference (4).
52) Ono, K., *Balancing of Flexible Rotor by Torque Excitation (Theoretical Research)*, Trans. JSME, (in Japanese), **50**-458, C (1984-10), pp.1790—1798.
53) pp.239—259 of reference (23).
54) Gasch, R. and Pfützner, H., *Dynamics of Rotating Shaft*, (Japanese Translation), Morikita Shuppan, (1978-10), pp.49—56.
55) pp.348—359 of reference (37).
56) Kato, M., Ota, H. and Nakamura, S., *Passing Problems of an Asymmetrical Rotor-Shaft through its First Critical Speed (Case of Constant Driving Torque)*, Proc. of IFToMM-jc Int. Symp. on Theory of Machines and Mechanisms, Nagoya, Japan, (1992-9), pp.515—519.
57) Kato, M., Ota, H. and Nakamura, S., *Whirling Vibration of a Shaft with an Asymmetrical Rotor in Passing through the Critical Speed (Case of Constant Driving Torque)*, Trans. JSME, (in Japanese), **59**-560, C (1993-4), pp.976—981.
58) Nakamura, S., Ota, H. and Kato, M., *Torsional Vibrations of a Rotating Shaft with an Asymmetrical Rotor while Passing through the Critical Speed of Whirling*, Trans. JSME, (in Japanese), **62**-597, C (1996-5), pp.1662—1668.
59) Nakamura, S., Ota, H. and Kato, M., *Torsional Vibration of an Asymmetrical Rotor-Shaft System after Passing its Critical Speed for Whirling*, Proc. of IMechE, 6th Int. Conf. on Vibrations in Rotating Machinery, Oxford, UK, (1996-9).
60) Kato, M. and Ota, H., *Whirling Vibrations of a Rotating Shaft with Load Torque (Instability due to Load Torque)*, Trans. JSME, (in Japanese), **56**-522, C (1990-2), pp.308—314.
61) Yamamoto, T. and Ota, H., *Dynamics of Machinery*, (in Japanese), Asakura-Shoten (1986-11), pp.238—240.